INTA	N.°	Pág.

EOARD-TR-85 09 (C)

(2)

AD-A159 927

Grant Number: AFOSR-83-0340.

DEFECTS AND MATERIALS CHARACTERIZATION BY ANALYSIS OF ULTRASONIC SIGNALS. STUDY OF A TECHNIQUE TO MEASURE ULTRASONIC ATTENUATION.

Carlos Valdecantos; José Miguel
Instituto Nacional de Técnica Aeroespacial (INTA)
Torrejón de Ardoz, Madrid, SPAIN.

Mayo - 1985

Final Report.

Approved for public release;
Distribution unlimited.

Prepared for:
AIR FORCE OFFICE OF SCIENTIFIC RESEARCH
Bolling AFB, D.C. 20332
and
EUROPEAN OFFICE OF AEROSPACE RESEARCH AND DEVELOPMENT
London, England.

EOARD-TR-85-09

20 AUG 1985

This report has been reviewed by the EOARD Information Office and is releasable to the National Technical Information Service (NTIS). At NTIS it will be releasable to the general public, including foreign nations.

This technical report has been reviewed and is approved for publication.

LARELL K. SMITH, Major, USAF
Chief, Physics/Physical Chemistry

ULTRASONIC CHARACTERIZATION OF MATERIALS

Contents

ULTRASONIC CHARACTERIZATION OF MATERIALS

1. Introduction. Nondestructive Testing

The objective of this work is to explore the actual possibilities of a NDT technique to be applied in laboratory conditions, as a first stage, in order to make measurements of mechanic and elastic parameters on metals.

Classic test of measurement of acoustic velocity and attenuation is useful to compute Young modulus or Poisson ratio, but these parameters have no wide technological usefulness. Much more interesting are others parameters such as yield strength, tensile strength, or fracture thoughness (K_{IC}). This is of particular interest in view of the cost of destructive test to asses it.

Up to date, critical part design is done taking tabulated data coming from handbooks, or destructive tests should be performed to have only a statistical estimation of the parameter. On the other hand, is out of possibilities to know positively the actual characteristics of a material in a critical area such as HAZ of a weld. It seems then justified to set up a technique able to measure technological parameters.

From the NDT techniques, ultrasonics seems, at a first look, a good way to intend. Ultrasonics is, first of all, a dynamic test because material is forced to transmit stress through the crystal structure.

As a first approximation it seems possible that some relation have to have between the ability of the material to withstand ambient stresses and its ability to transmit ultrasonic pulses without excesive loss of energy.

But, although this relation seems obvious, there is not, to our knowledge, a coherent theory supporting these empiric observations and, as a consequence, a model reasonably good cannot be established. Something can be done on monocrystals but common materials are full of grains, inclussions, obstacles in one word whose exact performance with elastic pulses is unknown.

An empiric approach is then needed in order to evaluate real attenuation of a material and to use it to estimate mechanical parameters.

Relative attenuation measurements with moderate precision is a usefull technique to evaluate the metallurgical quality of nodular irons and other materials, being able to estimate the strength of the material and to detect flaws at the same time. A similar technique is used to detect hydrogen attack in pressure vessels. In these examples relative attenuation measurements are taken and compared with those of samples with known condition.

This technique is not applied in thoughness or elastic parameters evaluation because absolute measurements are required and attenuation function, i.e. attenuation variation versus frequency, has to be calculated in order to deduce material characteristics.

Present work describes some experiments carried out at INTA's Ultrasonic Laboratory in order to set up a technique able to take absolute attenuation measurements over a range of frequencies from 15 to 60 MHz, typically. This range may seem too high if compared with conventional ultrasonic tests ranging around 4MHz, but in practice, this is still too low, being much more usefull to work in the range of several hundreds of MHz.

The reason is because for the ultrasonic pulse to interact with "accidents" such as grain limits, inclusions, microcavities, precipitates, etc., has to have a wave length of the same order of these accidents which is equivalent, in steel, to 600 MHz. (wave length: 0.01mm, similar to grain diameter for # 10 ASTM grain size). But attenuation at this high frequency is very strong and pulses will become completely cancelled out in a few tenths of a millimeter, too small to be the thickness of a sample to be characterized.

Working at 50MHz is easy to diferentiate several backwall echoes from several millimeters steel sample, but to estimate attenuation at 500 MHz extrapolation has to be performed and this is probably one of the main sources of errors of this technique as we will show in the experiments described later.

2. Theoretical study.

Attenuation measurements is based upon analysis of backwall echoes from plate parallel samples. Fig. 1a shows the technique with buffer, whose length is such that permits to have up to 4 backwall echoes from a 3mm thickness sample before 2nd interface echo. Two different interfaces exist: buffer-sample and sample-air.

Let:

zb = Acoustic impedance of buffer
zm = " " of sample
za = " " of air

$$zm \gg za \quad : \quad zm > zb$$

To solve the problem of calculate acoustic attenuation there are two techniques: the first one uses three echoes (interface buffer-sample and two backwall echoes); the other is based upon the analysis of the first two backwall echoes.

2.1 Three echoes method.

When a pulse is propagated from the buffer to the sample, is splitted off at the interface and some energy is reflected back to the transducer and the remainder goes into the sample through the interface. The amplitude of the reflected signal is the product of incident pressure times reflection coefficient for this particular interface. The phase is the same when the wave comes from a material with less acoustic impedance and is opposite in the other case.

Let the amplitude of initial pulse equal to unity.

Let:

R: reflection coeficient at the interface buffer-sample.

t: sample thickness.

: attenuation coefficient.

(R = 1 for sample-air interface)

At the position 1, fig. 1b:

Incident pressure: 1
Reflected pressure: R
Transmitted pressure: T

For the interface to be in equilibrium:

$$1 + R = T \qquad : \quad A = R \qquad (1)$$

Then, 1 + R is the pressure transmitted into the sample and is exponentially attenuated so that at the position 2 the amplitude is:

$$(1 + R)\, e^{-\alpha t}$$

Again, for the equilibrium of this position:

Incident pressure: $(1 + R)\, e^{-\alpha t}$

Reflected pressure: $(1 + R)\ e^{-\alpha t}$
Transmitted pressure: 0

At the point 3:

Incident pressure: $(1 + R)\ e^{-2\alpha t}$

Reflected pressure: $R\left[(1 + R)\ e^{-2\alpha t}\right]$

Transmitted pressure: B

$$B + R\,(1 + R)\ e^{-2\alpha t} = (1 + R)\ e^{-2\alpha t}$$

or:

$$B = (1-R^2)\ e^{-2\alpha t} \qquad (2)$$

In a similar way, at the point 5:

$$C = R\,(1-R^2)\ e^{-4\alpha t} \qquad (3)$$

From equations (1) to (3) one can calculate R and α.

Normalizing echoes by B:

$$A/B = \overline{A} = \frac{R}{1-R^2}\ e^{-2\alpha t} \qquad (4)$$

$$C/B = \overline{C} = R \cdot e^{-2\alpha t} \qquad (5)$$

From (4), (5):

$$R = \left(\frac{\overline{A}\cdot\overline{C}}{1+\overline{A}\cdot\overline{C}}\right)^{1/2} \qquad (6)$$

and: $$\alpha = \frac{1}{2t}\ln\left(\frac{R}{C}\right) \qquad (7)$$

Fig. 1 shows how echo A is phase-inverted with respect to echoes B and C. This implies a negative sign in (1) or in (2) and (3) but as long as we always work with power spectra, equation (6) and (7) may be considered valids. These equations may be applied to each frequency over the band of the transducer and this is the way to compute attenuation function (α versus frequency). A value of R is obtained for each frequency but these values do not differe much each other so that R may be considered as a constant over a wide range of frequencies.

If the attenuation is too high and C is too small considerable relative errors may occur. In this case use can be made of interface echo when the transducer is not coupled to the sample, the other two being buffer-sample interface echo and first backwall echo. References 7 and 10 to 12 examine equations and conditions such as thickness, acoustic velocity, reflection coeficient and other parameters in order to improve results.

2.2. Two echoes method.

This is the method applied by A. Vary and widely explained in references 7 including details about how to compute ultrasonic data.

The main problem in this technique is that reflection coeficient is unknown. Although acoustic impedances of buffer or sample are known, the true value of R cannot be calculated because coupling agent modifies the interface properties.

Then, we only can calculate upper and lower limits for R the first being that of interface coupling-sample:

$$R\ max = \frac{Zm - Za}{Zm + Za}$$

Zm: Acoustic impedance of coupling

Za: " " " sample

A-4902.3 Imprenta del INTA

The lower limit would be:

$$R\ min = \frac{Zm - Zb}{Zm + Zb}$$

Zb: Acoustic impedance of buffer.

For a usual frequency band, attenuation takes the form:

$$\alpha = A f^{M} \qquad (8)$$

where A and M are specific constant for each material.

By substituting (8) in (7) :

$$\frac{1}{2t} \ln\left(\frac{R}{C}\right) = A\ f^{M} \qquad (9)$$

In this equation R,A and M are unknowns, then an iterative method is applied as follows:

1. First backwall echo is isolated at the oscilloscope screen and digitized. The same is done with the second backwall echo.

2. Spectra of both echoes are computed and divided to obtain $\bar{C}$.

3. A reflection coeficient is suposed, i.e. Rmax .

4. By a least square method, the value of $1/2t \cdot \ln(R/\bar{C})$ is adjusted to a potential function $A.f^{m}$, computing by this way A and M.

5. With A and M, theoretical attenuation function $\alpha = A.f^{M}$ is calculated and compared with experimental $(1/2t \cdot \ln(R/\bar{C}))$ to estimate the fitting coefficient of the correlation.

6. R is decremented by a certain amount and steps 4 and 5 are again performed. If the new fitting coefficient is better than before one control is passed to step 6, otherwise R,A and M keep the old values.

To stop with computing, some of the two following conditions must be found:

a) That of preceeding paragraph.
b) A value of R greater than Rmax or smaller than Rmin is reached. This is cause of rejection of the calculus.

Calculus is also rejected if correlation coefficient is below a given one considered as a minimum (. 95 i.e.). Step 4 is performed over a range of frequencies around the control frequency of the spectrum, because low frequencies are diffraction affected and higer ones have low amplitude and relative errors may be excessive.

The way to define frequency band is that of the reference 7 , that is:

- Lower frequency limit: maximum of the first derivative of the spectrum of the 2nd backwall echo.
- Upper frequency limit: second maximum of the second derivative of the spectrum of the same echo.

This produces a fairly wide band and obviates the diffraction corrections at low frequencies.

3. Software.

A program to follow steps 1 to 6 of preceeding paragraph has been written for the Tektronix 4052 computer.

The structure of the program is as follows:

1. Main programm:

   It perform initiation and data capture. Several parameters must be imputed by the operator (Fourier transform limits and resolution, etc).

   Digitized waveforms are sent into the computer and the program goes to a loop to wait for a next operation.

2. Fourier transform:

   This routine calculates module and phase of Fourier integral of the waveform.

   Tektronix 4052 have a ROM-pack that performs FFT algorithm very quickly. But this implies that frequency resolution is inversely proportional to time resolution. In other words well defined time domain signals give poor spectra.

   To obviate this difficulty a chirp Z transform (CZT) algorithm has been written. It works very well but takes a lot of time to compute spectrum although not so much as DFT (Discrete Fourier Transform).

3. Compute derivatives:

   As before mentioned, two first derivatives of the spectrum of 2nd backwall echo are calculated to define limits of frequency.

4. Ratio of spectra:

Spectrum of the 2nd echo is divided by the spectrum of the first echo in order to calculate $\bar{C}$.

5. Fitting routine:

Performs the step described before (par. 2, steps 4 to 6).

6. Graphic plot:

A routine to plot curves on 4052 screen has been written and also another to have a copy on digital X-Y plotter.

7. Routine to restore:

Is a short programm that gives the menu when the main routine has been aborted.

8. There is also a command (via defined key) to break the programm when it is running.

9. A key is also defined to perform all the routines sequentially without any intermediate command.

4. Instrumentation.

Instruments used in experiments are listed as follows:

1. Ultrasonic Pulser-receiver Panametrics 5600 100 MHz bandwith.

2. Digital processing oscilloscope. Tektronix-7854, acquire repetitive signals, performs averaging and is able to transmit information to the computer via IEE 488 interface.

It has also several plug-in units such as:

- amplifier 7A16A
- time base 7B53A
- spectrum analyser (analog) 7L12
- digital delay 7D15

3. Probes:

Panametrics V358, 50MHz nominal frequency, and fused quartz buffer.

4. Computer:

Tektronics 4052, graphic desktop, 16 bit 64 Kb RAM computer.

Interface IEEE-488 for communication purposes.

5. Digital plotter Hewlett Packard 7470 A.

6. Printer. Facit 4510 matrix printer.

5. Experimental results.

Figs. 2 to 6 shows the effect of d.c. component on the spectrum.

Fig. 4 shows an echo and fig. 5 its expected spectrum.

Fig. 2 correspond to the same signal but with .04 volts of d.c. component. This is the cause of the appearance of the spectrum of fig. 3 (modulated), because Fourier integral is lineal. The spectrum of d.c. is that of fig. 5 because d.c. "exists" only within the time of oscilloscope window, and not from $-\infty$ to $+\infty$.

The way to get out d.c. components is to substract to the captured signal the value of the average of all the points (ref. 17).

5.1. First results.

Figs. 7 to 13 shows a characteristic test to compute attenuation function by two echoes method.

A carbon steel sample, 3mm thick and polished surfaces is used.

Valid zone to calculate attenuation is marked in figs. 8, 10 and 13 and corresponds to the first two derivative criterium (A. Vary).

The results for this particular test are:

- Valid zone: 19 to 42 MHz.
- Reflection coef.: 0. 849
- Fit: 0.9977
- M: 2.858
- A: $2.8565.10^{-6}$
- $\alpha = 2.8565.10^{-6}. f^{2.858}$

Figs. 14 and 15 show the first backwall echoes and its spectra for a quenched steel and figs. 16 and 17 the same for annealed condition.

It is easy to see how different are the spectrum of both samples; maxima being closer in the quenched sample, in both amplitude and frequency.

Then, qualitative results are as expected. Let us see quantitative ones:

Quenched sample:

- Valid zone: 22 to 47 MHz.
- Reflection coeff.: 0.899
- Fit: 0.991
- M : 1.91
- A : $4.05.10^{-5}$
- $\alpha = 4.05.10^{-5}. f^{1.91}$

Annealed sample:

- Valid zone: 17 to 41 MHz.
- Reflection coeff.: 0.840
- Fit: 0.996
- M : 3.14
- A : $4.87 . 10^{-7}$
- $\alpha = 9.87 . 10^{-7} . f^{3.14}$

At first glance it may seem that these results are good enough but several objections can be made:

1. Parameter A is greater in the quenched sample and this implies that at low frequencies attenuation will be greater than in annealed sample. This occurs up to about 20 MHz.

2. Fitting is a little low if compared with those of ref. 7.

3. Reflection coefficient varies too much from one sample to another, and this is not easy to explain on the basis of acoustic impedance differences.

   It seems also that reflection coefficient is too high. A good value would be 0.6 to 0.7.

4. Results for M are too low if compared with those of the available literature.

5. Valid zone, 20 to 45 MHz, is narrower than those of references (20 to 60 MHz or even more).

6. If the curve f → ratio of spectra is presented in a logarithmic plot a straight line should be drawn having a slope equal to M.

$$\log 1/2t \cdot \ln \left(R/\bar{C} \right) = \log C + M \log F \qquad (10)$$

Fig. 18 shows this result for the quenched sample. Curve is far from straighteness and this may be the reason of the low fitting value. Fig. 19 shows the same effect for the annealed sample.

All these objections point out that there are some problems that are more obvious when experiment is repeated many times.

The table that follows gives the results for M for 10 experiments carried out without moving the transducer nor instrumentation controls. This is only sucessive digitizations of the same signal.

Test	M	Test	M
1	5.15	6	4.92
2	4.69	7	4.30
3	4.59	8	4.52
4	3.87	9	4.44
5	4.97	10	5.49

Average value: 4.69
Standard devia. 0.43

This represents a great spreading of results and overlapping between low values for annealed sample and high values for quenched sample may in fact occur.

Spreading causes a great trouble and masks the effects of other disturbances such as electronic distortion of signals or diffraction effects.

This is because main effort of this work has been directed towards the study of the causes of the lack of repeatability of results, forgetting for the moment the absolute value of the parameters.

A-4(10)2.3 Imprenta del INTA

5.2 Noise.

Figs. 20 and 21 show two sucessive digitalizations of the same signal in the following conditions:

- Horizontal scale: 20 nanosec./div.
- Vertical scale: 100 milivolts/div.
- 128 points/waveform.
- Averaging: 10 samples (on the oscilloscope).
- Attenuation: 22 dB.

For the spectrum conditions are:

- Frequency band: 0 to 100 MHz.
- Resolution : 129 points.

There is in both echoes a visible oscillation overimposed to the signal. This affects all the waveform although it is more perceptible where the signal is near zero volts amplitude. This is the noise coming mainly from digitization process. It would also be possible to come from electric noise but in this case oscillation would appear in fig. 21 a which is an analog representation of the signal over the digital oscilloscope screen. If one takes several digitizations from the same signal and observs the value of a particular point near the maximum of the signal, ten sucessive catching give the following results:

Test no.	Volts	Test no.	Volts
1	0.5567	6	0.5511
2	0.5493	7	0.5505
3	0.5554	8	0.5548
4	0.5609	9	0.5342
5	0.5511	10	0.5591

Average value: 0.5543
Standard deviation 0.00367
Maximum: 0.5609
Minimum: 0.5493

Difference between extremes is 0.012 or 1.2 per cent over the average.

If the point of the signal has a value closer to zero the results are:

Test no.	Volts	Test no.	Volts
1	0.2441	6	0.2374
2	0.2295	7	0.2289
3	0.2258	8	0.2283
4	0.2368	9	0.2277
5	0.2368	10	0.2332

Average: 0.2328
Standard deviation: 0.00549
Maximum: 0.2441
Minimum: 0.2258

Here the difference is about 4.7 per cent.

Given that absolute error of digitization is the same for all the screen, relative error will decrease for greater voltage in the signal concluding that it is better to work with signal of maximum amplitude (full screen high).

Let us see now how 7854 oscilloscope captures signals and how the noise is produced. This apparatus acquires repetitive high frequency signals and take random samples along a certain amount of time. Numbers of averaging (1 to 1023) is imputed from the keyboard or by programme together with the digitization command.

As averaged samples increase the digital value approaches to analog signal. But time to acquire signal is also increased.

The 7854 has 10 bits resolution, in other words it only can represent 1024 different states (voltages) and because of this, quantization error is produced.

Length of words is 14 bits for the 7854 oscilloscope and one can reach this higher precision averaging 32 samples. It is still possible to raise precision if samples are averaged in an external computer with, for example, 16 bits words.

Time base jitter is also a source of errors. Jitter causes signal to move very quickly along time base and is caused by unstabilities of triggering.

Another noise source is electric noise from cables, amplifiers, etc., and is already present in analog signals.

Total amount of noise is the sum of quantization, jitter and electric noise.

5.3. Signal averaging.

For repetitive signals the easiest way to reduce noise is to average many signals. Fig. 22 shows a smooth signal acquired by averaging 150 samples and contrasts with fig. 21 acquired with only 10 samples. In this last example, noise is clearly visible.

The question is how many signals have to be averaged to reduce noise up to acceptable limits. If the noise is ramdom, signal to noise ratio raises with the square root of the number of samples. Then if a signal to noise ratio is given is a simple matter to calculate the number of samples to be averaged to reach another ratio. The slope of the curve of square root is high for low values, so that noise falls quickly with first averages but many are after needed to have only little improvements in signal to noise ratio. If signal to noise ratio is 1, the following applies:

Samples Averaged	Signal/Noise
1	1
10	3.16
100	10
1000	31.6

Increasing averaged samples by a factor of 100, signal to noise ratio increases by 10 in accordance with square root law. The trouble is that this only applies to random noise and probably noise has several components other than random. Still we have the finite number of bits of A/D converter.

To evaluate experimentally the noise time base without any signals was acquired in different conditions. In the table that follows figures indicate the average of absolute values of the signal acquired.

nr. signals averaged in the computer

signal averaged in oscilloscope	1	5	10	30	50	70	90	110	150	250	500	1200
2	45	19	14	9	7	8	--	6	--	5	--	--
5	31	15	10	7	6	5	5	-	5	5	--	--
7	26	11	9	6	6	6	-	5	-	5	--	--
10	19	11	7	5	4	4	4	-	-	-	4	4
30	15	5	4	4	3	3	3	3	3	3	--	--
50	13	4	3	4	3	3	3	-	3	2	--	--
70	12	6	5	3	3	2	2	2	2	2	--	--
90	9	5	4	4	3	3	3	-	3	-	--	--
250	9	4	4	3	3	-	4	-	-	-	--	--

Fig. 23 shows a plot of some of the rows of this table, and it is easy to see that when the number of samples averaged in oscilloscope raises a certain value, noise falls only very little, and is better to start with computer averaging, although time increases. Finally it was decided to average 30 signals in oscilloscope and to take another 30 of this signals to average in the computer. This is a practical limit because the whole acquisition process last about 6 minutes (with 20 nanoseconds/ div and a p.r.f. of 10 KHZ).

In these conditions, a signal with maximal deviation of 1 to 5 percent can be acquired. It is still surprising that such a little difference be the origin of the great dispersion of the results. It should be remembered that standard deviation is about 20 per cent for parameter M and still worse for A.

If the experiment of paragraph 5.1 is repeated for the quenched sample but with 100 averaging instead of 10 in the intervall of M = 2.3 to M = 2.6 there are 36 of the 50 values (remember that in the case of 10 averaging only 13 results fall into this intervall).

5.4. Averaging of spectra.

From the theoretical point of view the results of averaging spectra or averaging signals must be equivalent if the number of sample is the same.

Discrete Fournier transform is expressed by:

$$X_d(K) = \sum_{n=0}^{N-1} X(n)\, e^{-j2\pi nK/N}$$

for K = 0, 1. 2 ... N/2

where:

$X_d(K)$ = Coefficient of the spectrum.

$X(N)$ = Discrete amplitude of the signal from which the spectrum is calculated.

N = Points per waveform.

If, to acquire X(n), M samples are averaged:

$$X(n) = \frac{1}{M} \sum_{i=0}^{M-1} X_i(n)$$

Substituting in the prior expression:

$$X_d(K) = \sum_{n=0}^{N-1} \left(\frac{1}{M} \sum_{i=0}^{M-1} X_i(n) e^{-j2\pi nK/N} \right.$$

$$= \frac{1}{M} \sum_{n=0}^{N-1} \sum_{i=0}^{M-1} X_i(n) e^{-j2\pi nK/N}$$

or:

$$X_d(K) = \frac{1}{M} \sum_{i=0}^{M-1} \left(\sum_{n=0}^{N-1} X_i(n) e^{-j2\pi nK/N} \right)$$

expression that corresponds to the averaging of M spectra. To show how this theory results in practice some experiments were performed having in mind that limited speed of our computer in computing FFT strongly reduces the practical possibilities of this technique. An experiment in which averaging of 20 spectra from signal acquired with 30 averaged samples gave the following results:

	M	Reflection coeff.
Average value	2.42	0.603
Standard deviation	0.38	0.016
Maximum value	3.56	0.63
Minimum value	1.79	0.57
per cent deviation to the average (max)	47	4.5
percent deviation to the average (min)	26	5.5

A-4/602.3 Imprenta del INTA

Results are similar to that of signal averaging and although more experiments should be realized, it seems that no significant improvement will be obtained with this technique.

5.5. Considerations about noise and its spectrum.

Fig. 24 shows a computer generatedrandom noise and Fig. 25 its spectrum. Average of absolute value for this signal is $2.567.10^{-4}$, but average of spectrum is 2.10^{-3} i.e. the noise in the spectrum is about 10 times greater than that of the signal. Modulation of spectrum is related with oscilloscope time window. In this case is 200 nanoseconds which is equivalent to 5MHz where the first peak of the spectrum is. This is also the band limit for low frequencies. Setting time base to 100 nanoseconds the numbers of peaks of the spectrum is also reduced by one half approx. These peaks, that are convolved with the spectrum of the signal, results from the time domain multiplication of an infinite signal with a square time window having an amplitude of unity during the oscilloscope time window and zero out of this limit.

Fig. 26 shows time base captured with 10 averages. Fig. 27 corresponds to its spectrum and looks like fig. 25. Again spectrum noise (10^{-2}) is one order of magnitude greater than that of the signal (9.10^{-4}).

Fig. 28 was obtained as that of fig. 26 but 50 averages and then noise goes down to 3.10^{-4}. Its spectrum (fig. 29) is similar to the before mentioned except for that first peak has a greater amplitude.

Fig. 30 has been obtained by overlapping 50 spectra equivalents to that of fig. 29. First peak is clearly noted both in amplitude and frequency, others being randomly distributed.

If 50 spectra from computer generated random noise are overlapped no outstanding peak appears as is shown in fig. 31.

If many samples are averaged (50 x 50 samples) time base appears as shown in fig. 32. There is in fig. 31 an apparent distortion of the time base which is clearly present in figs. 26 and 28 but hidden because higher noise level. If period of the signal is about 200 nanosecs. its corresponding frequency is 5MHz, i.e. that of the peak of first maximum in fig. 33.

From paragraph 5.3 the parameter used to estimate noise is the average of absolute values of the noise. Let us suppose that noise is fully cancelled; then the average of absolute values would correspond to the average of the distortion of true base and this is because averaging does not cancell noise as expected. When noise level is high, distortion influence is of no importance, the contrary applies if noise level is low, i.e. many samples are averaged.

Let us propose a numerical example:

Let R1 be the noise in signal 50 averaged samples.
Let R2 be the noise in signal 2500 averaged samples (50 x 50) then:

$$R2 = R1\sqrt{\frac{50}{2500}}$$

if "a" is the average value of the distortion:

$a + R_1 = 3.27 \cdot 10^{-4}$ (parameter value for 50 averaged signals)

$a + R_2 = 1.36 \cdot 10^{-4}$ (" " " 2500 averaged signals)

Solving for a R1 and R2

$$a = 1.05.10^{-4}$$

$$R1 = 2.22.10^{-4}$$

$$R2 = 0.52.10^{-4}$$

These results affects those of the table in paragraph 5.3. Figs. 34 to 39 corresponds to 26 to 29, 32 and 33. Differences are that in last ones the time base captured is between two succesive backwall echoes.

If the same signal is captured several times and spectrum are computed, quotient of this spectra should be equal to unity. Fig. 40 shows this kind of experiment performed many times. It is evident that dispersion is much higher in low and high frequency bands.

This demonstrates that separation of effects of errors in the technique and repeatability is not possible. If something is wrong in the method applied results obtained will repeat, although they may be false. But if, for example, a wrong band of frequency is selected, results not only would be false but also it will appear a severe lack of repeatability.

Fig. 41 is similar to fig. 40 but a signal with jitter is used. The results show much more dispersion in the whole frequency band. Let us see how the noise affects the results. If a random noise is added to spectra and parameter M is calculated the results, are shown in the following table for several noise levels.

Parameter M	Noise level (volts) 0.005	0.0005	0.00005	0.000005
Average	1.53	2.224	2.283	2.2843
Standard deviation	0.7	0.1	0.002	0.0002
Maximum value	4.62	2.73	2.2883	2.2848
Minimum value	0.36	1.99	2.2791	2.2839

Standard deviation of 0.7 is quite rejectable. If one intends to pass from 0.1 to 0.002 average of 100 times samples are needed . For a standard deviation of 0.1 we have found that 1000 samples are enough good. But to reach 0.002 we would need 100000 samples being quite impossible for our instrumentation.

5.6 Influence of jitter.

Figs. 40 and 41 show influence of jitter on the repeatability. Fig. 42 shows an echo with jitter and steps are clearly visible. Error induced by jitter are proportional to the slope of the signal and as a consequence error is not the same for all the points of the signal. If signal with jitter is captured two succesive times and difference of both signals is computed the results shown in figs. 43 to 45. The difference looks like derivative of the signal if there is jitter. Results of 50 experiments with signals with jitter are reported in the following table:

	Reflection coef. (R)	Parameter M	Parameter A
Average value	0.6107	2.646	$7.65.10^{-6}$
Standard dev.	0.016	0.1562	$5.39.10^{-6}$
Maximum value	0.6605	2.93	$3.04.10^{-6}$
Minimum value	0.5800	7.24	$2.02.10^{-6}$

Relative error for R is about 2.5% and 6% for M but is as high as 70% for A.

If jitter is cancelled out and experiment is again performed, other conditions being constant, the results are:

	Reflect. coef. (R)	Parameter M	Parameter A
Average value	0.6187	2.384	$1.77.10^{-5}$
Standard dev.	0.0051	0.0381	$2.49.10^{-6}$
Maximum value	0.627	2.516	$2.25.10^{-5}$
Minimum value	0.603	2.314	$1.007.10^{-5}$

Now dispersion for R is about 0.8%, 1.8% for M and 15% for A, which is about 3.5 times better than if jitter is present.

5.7. Three echoes method. Study of dispersion.

In the two echoes method there are only one equation for two unknowns, then some aprioristic evaluation of R have to be done. (See para. 2). Because of this is possible to assign some of the amount of dispersion to this factor. To see how three echoes method compares with, both technique have been applied to the same digitized signals previously captured and stored in tape.

All the signal in this experiments are with some jitter because there is no way to acquire interface echo without a precision external trigger source and there are not in our Laboratories such an equipment.

Fig. 46 to 51 show interface echo and first two backwall echoes with its spectra.

Results obtained were:

	Reflect. coef (R)	Parameter M	Parameter A
Average value	0.9589	2.425	$1.43.10^{-5}$
Standard dev.	0.0012	0.049	$2.67.10^{-6}$
Maximum value	0.9615	2.517	$2.21.10^{-5}$
Minimum value	0.9557	2.307	$1.01.10^{-5}$

Standard deviation is lowered if compared with two echoes method. A variation on this technique is to compute R and α by equation (6) and (7), (para. 2). The following applies:

$$\alpha_1 = A f_1^M$$

$$\alpha_2 = A f_2^M$$

This equation can be solved by A and M. If this is computed for many pairs (α_1, f_1) and (α_2, f_2) inside valid frequency band many values for A and M are obtained an averaged to compute final values. If this is done for the same signals as the preceeding case one obtains:

	Attenuation (α)	Parameter M	Parameter A
Average value	0.0462	2.892	$5.05.10^{-6}$
Standard deviat.	$5.35.10^{-4}$	0.051	$1.13.10^{-6}$
Maximum value	0.0491	3.012	$9.14.10^{-6}$
Minimum value	0.0453	2.721	$3.06.10^{-6}$

Deviations are comparable to the preceeding experiment or, in some cases still higher. A column with attenuation is plotted showing an error of 1% with respect to average. It seems that this variation do not contribute to improve results.

5.8 Influence of truncation of time domain signals.

Truncate signals is to make cero all the elements of digitized signal that are out of the five main oscillations.

Fig. 52 to 57 are the signals of preceeding paragraph but truncated. Its spectra are wider as can be expected.

Results obtained with these signals, and two echoes method are:

	Reflect. coef. (R)	Parameter M	Parameter A
Average value	0.8827	3.972	$4.92.10^{-8}$
Standard dev.	0.0047	0.050	$8.99.10^{-9}$
Maximum value	0.8904	4.083	$3.21.10^{-8}$
Minimum value	0.8675	3.875	$7.81.10^{-9}$

Error in R is about 0.5%, 1.25% for M and 18% for A. Results are as good as those from three echoes method with captured signals.

The same experiment with three echoes method are:

	Reflect. coef. (R)	Parameter M	Parameter A
Average value	0.9592	2.554	$9.21.10^{-6}$
Standard dev.	0.0012	0.055	$2.013.10^{-6}$
Maximum value	0.9617	2.647	$1.72.10^{-5}$
Minimum value	0.9565	2.380	$6.43.10^{-6}$

Deviations are 0.1%, 2% and 22%. These results show that three echoes method do not improve results if truncated signals are used.

Finally, two echoes method is applied to jitter-free truncated signal.

	Reflect. coef. (R)	Parameter M	Parameter A
Average value	0.8791	3.969	$5.04.10^{-8}$
Standard dev.	0.0092	0.029	$6.84.10^{-9}$
Maximum value	0.8977	4.040	$6.36.10^{-8}$
Minimum value	0.8592	3.913	$3.68.10^{-8}$

Errors are 1%, 0.7% and 13%, being the best result obtained up to now from the point of view of repeatability.

Some preliminary conclusion can be drawn from the experiments:

1. Repeatability increases with jitter-free signals.
2. If there is jitter and signals are processed as raw signals best results are obtained with three echoes method.
3. If there is jitter and signals are truncated both three and two echoes techniques give similar results
4. With jitter-free and truncated signals best absolute results are obtained.

Another series of interesting experiments were performed in order to evaluate how the displacement of signal along the window affects the spectrum.

Let us see the following experiment:

1) 30 x 30 samples are averaged on oscilloscope and computer and spectrum is computed.

2) Some points from the leading of the waveform matrix are rotated to the trailing edge of the matrix, and amplitudes are kept constant. This causes an efec-

tive digital displacement of the signal.

3) Spectrum of translated signal is computed and substracted from the spectrum of original signal. Average of absolute values of difference is computed.

If one point is rotated, average is about 0.0005 raising to 0.002 if rotations is performed over 12 points.

If the signal is truncated prior to translation, differences fall down to 1.5×10^{-14} for 1 point rotation or 2.37×10^{-4} for 12 points.

When truncated waves are used error is without signification, but with raw signals error is about the same of that causing the lack of repeatability as beforementioned.

Figs. 58 and 59 show the echo and its spectrum. Fig. 60 shows the same signal after being 12 points displaced, and fig. 61 its spectrum. Figs. 62 to 65 are similar, but with truncated wave.

5.9. Influence of signal digitizing equipment.

Let us see how equipment influences repeatability.

Tektronix 7912-AD is a high frequency digital transient records, able to capture signals in a single sweep. It has a matrix diode, 512 x 512 points that become charged when electron beam sweeps time base. Another beam is used to "read" the matrix and average vertical axis values are stored to be processed.

This is an intrinsic jitter-free very fast technique. With repetitive signals it can perform average of 64 signals in less than 1 second.

By courtessy of Spanish agent of Tektronix we had the opportunity to work with this equipment along a week.

With 100 averaged signals repeatability was the same as obtained with 30 x 30 signals in 7854 oscilloscope. Although no particularly good results were obtained, time to perform experiments was much lower. This clearly indicates that sources of error are present other than those coming from digitizing equipment.

6. Finding actual magnitude of unknowns.

Up to now it has been shown that parameters take very spreaded values, and how with some variation in technique a substantial reduction of the spread band had been accomplished, but evaluation of actual magnitude still remains.

To do this, one of the main jobs is to select, mannually or automatically, the frequency band along which curve fitting will be performed. This curve must have enough frequency range and should be straight when a logarithmic scale is used (see para. 5.1).

This last condition is very important but, unfortunately we have not achieved up to now in a satisfactory manner. All the figures found look similar to that of figures 18 and 19.

This problem may be related to possible lack of linearity or distortion caused by receiver equipment. In fact we never can found echoes such as those of ref. 7, whose symetry is almost perfect.

The pulse output of our Panametrics - 5600 falls with some ringing, probably because impedance matching. We have observed too that beyond 30 MHz linearity of amplifier falls below 3dB tolerance.

Damping potentiometer is also very critical and much care should be taken in its use to avoid lack of repeatability.

Time stability is very important in order to compare results. We have found that this is a significative shifting of amplitude of signals up to four hours after equipment has been powered up.

A list of possible sources of error are given in ref. 7 and may be:

- Defects in the buffer or in the piezoelectric oscillator.
- Improper impedance matching.
- Trailling oscillations; improper backing.
- Lack of uniformity in coupling or lack of pressure between sample and transducer.
- Alinearities in amplifier stages.
- Digitizing alinearities.
- Flaws of defects in the sample material. Bad surface finish. Lack of parallelism between faces.

Some distorsion may also be occured at computer stages. Signal truncation is the result of multiplying raw signal by a window, whose spectrum is involved with that of raw signal. This way true raw signal spectrum is unknown and best results are in some way less true.

To supress d.c. components we perform a substraction of the average value of the signal from every point in the array. But if raw signal is such that positive peaks do not balance negative ones the average may not be equivalent to d.c. component. Sometimes average of, say, 20 point of leading or trailing adges of raw signal is substracted from the signal.

Diffraction corrections performed in some cases have not given expected results.

7. Summary.

Compute attenuation function without significative errors is not an easy problem. If parameters A and M are to be calculated from the attenuation data, difficulties increase.

To evaluate yield point and fracture toughness by non-destructive ultrasonic technique attenuation at high frequencies have to be calculated (i.e. 300 - 400 MHz). As long as these frequencies are by no means transmitted through any common materials, one is forced to extrapolate data obtained at much lower frequencies (10 - 50 MHz). This is the way because very little errors in experimental measurements become amplified and make results virtually unacceptable.

Let:

$$\alpha = A \cdot f^{M}$$

taking differentiation

$$d\alpha = \frac{\partial \alpha}{\partial A} dA + \frac{\partial \alpha}{\partial M} dM$$

$$\frac{\partial \alpha}{\partial A} = f^{M} \quad ; \quad \frac{\partial \alpha}{\partial M} = M \cdot A \cdot f^{M-1}$$

$$d\alpha = f^{M} dA + AMf^{M-1} dM$$

$$\Delta\alpha = f^{M} \Delta A + AM f^{M-1} \Delta M$$

if following tipical values are supposed:

$M=3$
$A=5.10^{-6}$
$f=300MHz$
$\Delta M=3\%$
$\Delta A=13\%$

this error is too big to accept such measurement. Such an error may be induced by one or both of two following sources:

- Error from Fourier Integral approximation.
- Errors from equipment.

Errors coming from computer stages are due to discretization of a continuous function. Its magnitude may be mathematically predicted and does not have any influence on repeatability.

Errors from equipment come from data capture or from transmit-receiver stages unstabilities (jitter, electronic noise), amplifier lack of linearity, improper impedance matching or improper surface finished samples.

Improvements have been achieved by averaging, using jitter-free signals, three echoes technique and truncation of raw signals.

Other possible way to improve results is to set time base and amplifier controls so that signal occupes maximum width and heigh of the screen. In high frequency signals this may cause some jitter because time base sweeping control knobs limits may be reached.

Further work will be performed in order to implement noise suppression algorithms.

To our knowledge, the main obstacle is to suppress amplifier aliniearities and to improve impedance matching.

8. Conclusions.

Absolute cuantitative ultrasonic attenuation measurements is considered as a fundamental approach to materials characterization and nondestructive evaluation of technological parameters.

However, setting up a suitable procedure to perform such measurements seems not a trivial problem because errors may produce unacceptable spreading of results. Little errors in the testing frequency band become multiplied because extrapolation to much higher frequency is to be performed.

Factors affecting results are:

- Noise from digitizing process and/or analog instruments.
- Lacks of linearity in ultrasonic transmit-receiver and/or transducers.
- Irregularities in the transducer-sample coupling.

Further effort will be devoted to study and avoid disturbing effects caused by these variables.

Acknowledgements

This research was partially supported by European Office for Aerospace Research and Development under contract EOARD - 82055.

REFERENCIAS

1 - Vary, Alex. "Concepts and Techniques for Ultrasonic Evaluation of Material Mechanical Properties", tomado de: Mechanics of Non Destructive Testing (1980), Editado por W.W. Stinchcomb.

2 - Vary, Alex. "Correlations Between Ultrasonic and Fracture Toughness Factors in Metallic Materials", Fracture Mechanics, ASTM STP 677, C.W. Smith, Ed. American Society for Testing and Materials, 1979, pp 563-578.

3 - Vary, Alex. "Correlations among Ultrasonic Propagation Factors and Fracture Toughness Properties of Metallic Materials", Materials Evaluation, Vol. 36, nº 7, 1978, pp 55-64.

4 - Vary, Alex. "Quantitative Ultrasonic Evaluation of Mechanical Properties of Engineering Materials", National Aeronautics and Space Administration, TM-78905.

5 - Vary, Alex. "Correlations Between Ultrasonic and Fracture Toughness Factors in Metallic Materials", National Aeronautics and Space Administration, TM-73805, 1978.

6 - L.S. Fu, "On Ultrasonic Factors and Fracture Toughness", Engineering Fracture Mechanics, Vol. 18, nº 1, pp 59-67, 1983.

7 - Vary, Alex. "Computer Signal Processing for Ultrasonic Attenuation and Velocity Measurements for Material Property Characterization", National Aeronautics and Space Administration, Technical Memorandum 79180, 1979.

8 - Francisco Ramirez Gómez y otros, "Introducción a los Métodos de Ensayos No Destructivos de Control de la Calidad de los Materiales". Editado por Instituto Nacional de Técnica Aeroespacial "Esteban Terradas", Madrid, Segunda Edición, 1978.

9 - Krautkrämer Josef and Herbert. "Ultrasonic Testing of Materials", Second edition, Springer-Verlag, Berlin, Heidelberg, New York, 1977.

10 - Papadakis, E.P. "Buffer-Rod System for Ultrasonic Attenuation Measurements", the Journal of the Acoustic Society of America, Vol. 44, no. 5, pp 1437-14441, 1968.

11 - Papadakis, E.P., Fowler, K.A. and Lynworth, L.C. "Ultrasonic Attenuation by Spectrum Analysis of Pulses in Buffer Rods: Method and Diffraction Corrections The Journal of the Accoustic Society of America, Vol. 53, no. 5, pp 1336-1343, 1973.

12 - Papadakis, E.P., Lynnworth, L.C., Fowler, K.A. and Carnevale, E.H. "Ultrasonic Attenuation and Velocity in Hot Specimens by the Momentary Contact Method with Pressure Coupling, and Some Results on Steel to 1200ºC The Journal of the Acoustical Society of America, Vol. 52, no. 3, pp 850-857, 1972.

13 - Papadakis, E.P. "Ultrasonic Diffraction Loss and Phase Change in Anisotropic Materials", The Journal of the Acoustical Society of America, vol. 40, no. 4, pp 863-873, 1966.

14 - Hajime Seki, Andrew Granato and Rohn Truell, "Diffraction effects in the Ultrasonic Field of a Piston Source and their Importance in the Accurate Measurement

of Attenuation", The Journal of the Acoustical Society of America, Vol. 28, no. 2, pp 230-238, 1956.

15 - G.C. Benson and Osamu Kiyohara, "Tabulation of Some Integral Functions Describing Diffraction Effects in the Ultrasonic Field of a Circular Piston Source", Journal of the Acoustical Society of America, Vol. 55, No. 1, pp 184-185, 1974.

16 - Papadakis, E.P. "Correction for Diffraction Losses in the Ultrasonic Field of a Piston Source", The Journal of the Acoustical Society of America, Vol. 31, No. 2, pp 150-153, 1959.

17 - Ramirez, R.W. "The FFT: Fundamentals and Concepts", Tektronix, Inc. Beaverton, Oregon, 1975.

18 - Alan V. Oppenheim and Ronald W. Schafer, "Digital Signal Processing", Prentice-Hall, Inc., Englewood Cliffs, New Jersey, 1975.

19 - Lawrence R. Rabiner and Bernard Gold, "Theory and Application of Digital Signal Processing", Prentice-Hall, Inc., Englewood Cliffs, New Jersey, 1975.

20 - Cochran, W.T., Cooley, J.W., Favin, D.L. and others, "What is the Fast Fourier Transform?", IEEE Trans., Audio Electroacoustic, Vol. AU-15, pp 45-55, 1967.

21 - Bergland, G.D. "A Guided Tour of the Fast Fourier Transform", IEEE Spectrum, Vol. 6, pp 41-52, July 1969.

22 - "FFT Algorithms Speed Digital Signal Processing", Electronic Design, July 5, 1980, pp 111-118.

23 - Rabiner, L.R., Schafer, R.W. and Rader, C.M. "The Chirp Z-Transform Algorithm", IEEE Trans. Audio Electroacoustic, Vol. AU-17, pp 86-92, 1969.

24 - Rabiner, L.R., Schafer, R.W. and Rader, C.M. "The Chirp Z-Transform Algorithm and Its Application", Bell Sys. Tech, J. Vol. 48, pp 1249-1292, 1969.

25 - "Chirp Z-Transform", Enviado por Christophe Flateau de Tektronix Europe B.V.

26 - Flateau Christophe, "Use of Waveform Digitizers for Ultrasonic Characterization of Materials and Tissues Part 1", Tektronix Europe B.V. Technical Note EA45TN-002.

27 - Clark Fuley, "GPIB Communication with the 7854", Tektronix, Beaverton. Oregon, 1980.

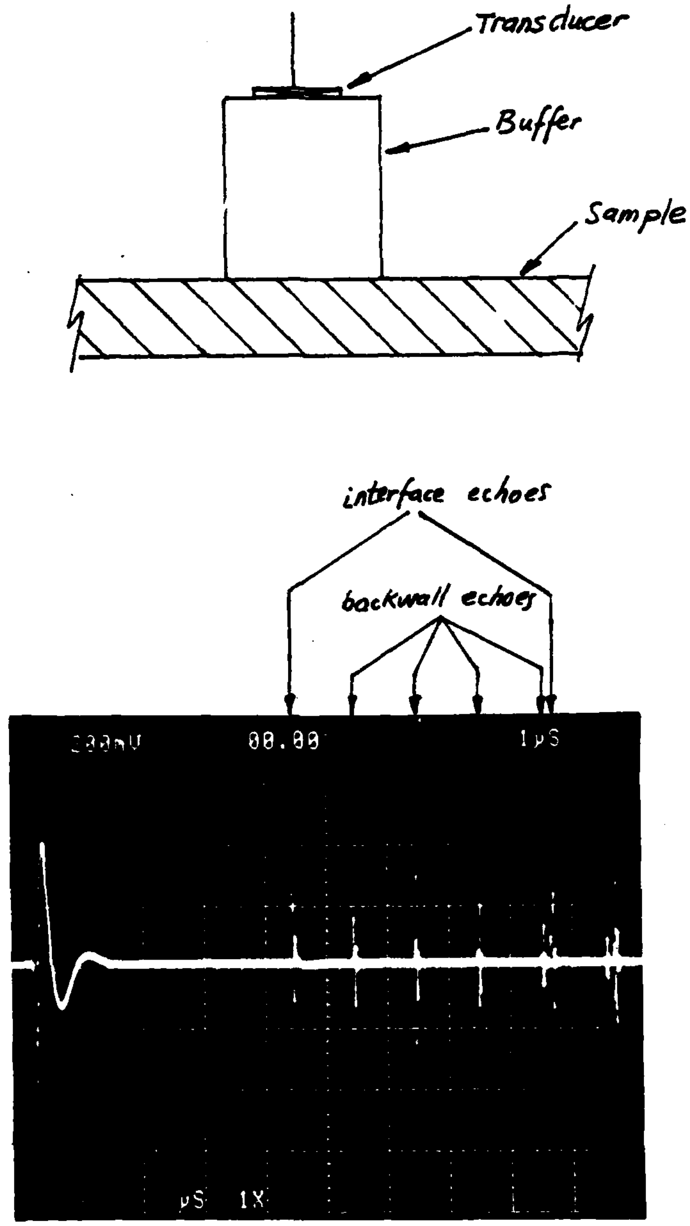

Fig. 1 (a) Tests technique (schematic)

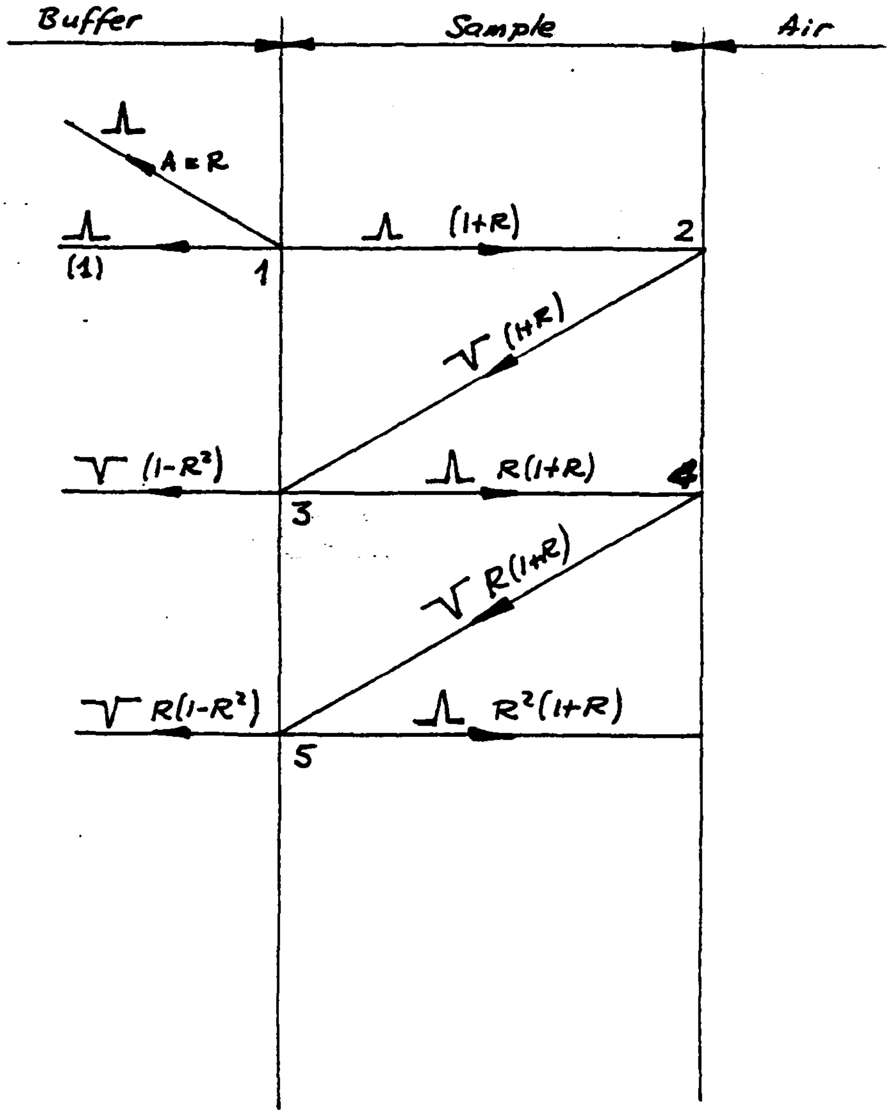

Fig. 1 (b)
Relationship between reflections inside sample.

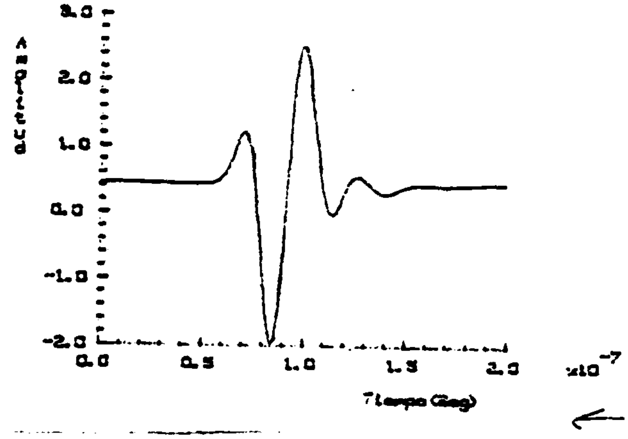

Fig. 2 signal with d.c. component.

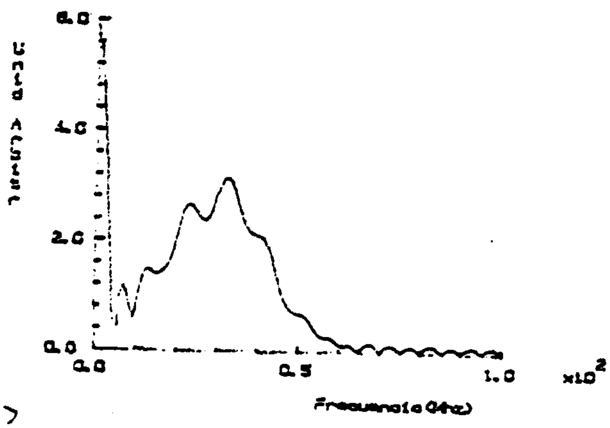

Fig. 3
Spectrum of signal of fig. 2.

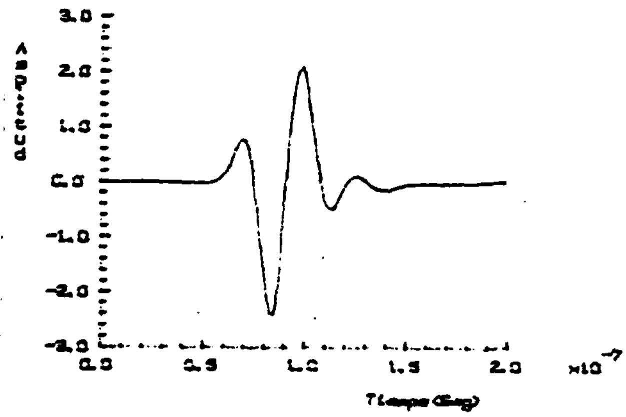

Fig. 4
Signal without d.c. component.

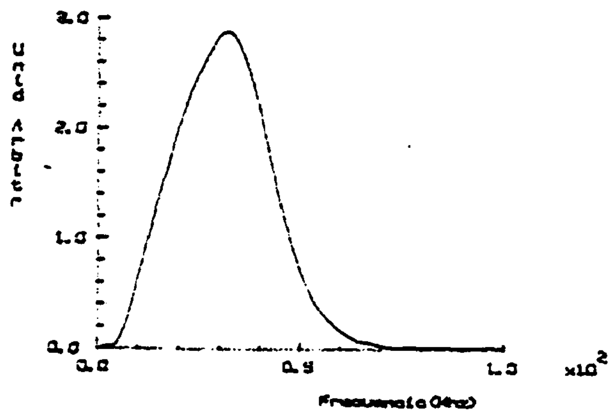

Fig. 5
Spectrum of the signal of fig. 4.

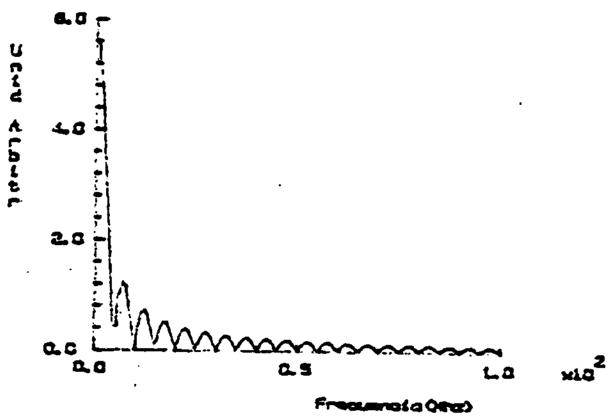

Fig. 6
d.c. signal spectrum.

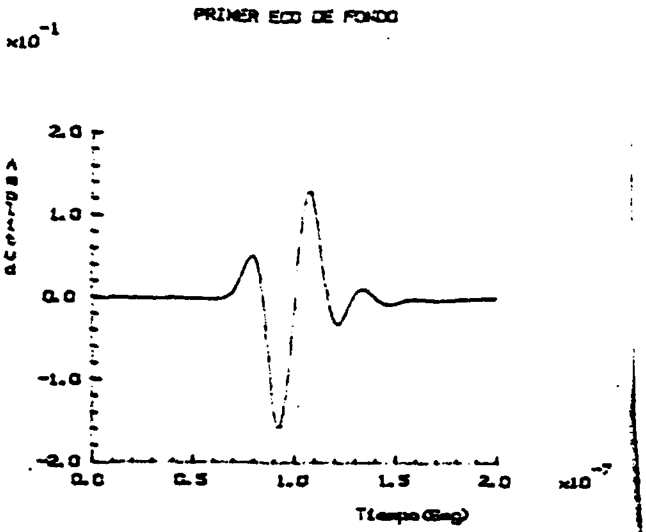

Fig. 7
Steel sample. 1st backwall echo

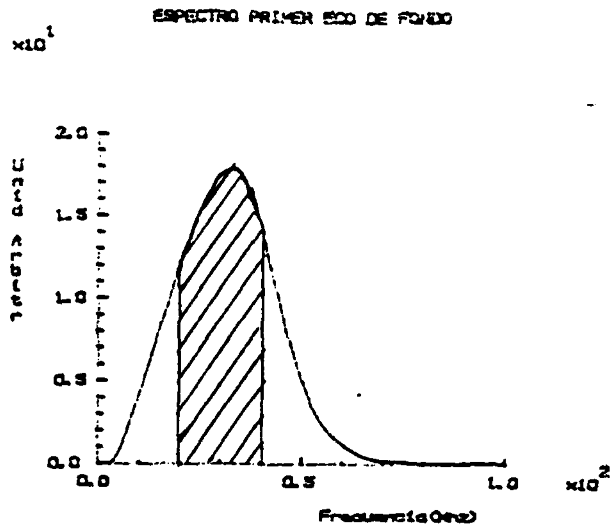

Fig. 8
Spectrum of signal of fig. 7

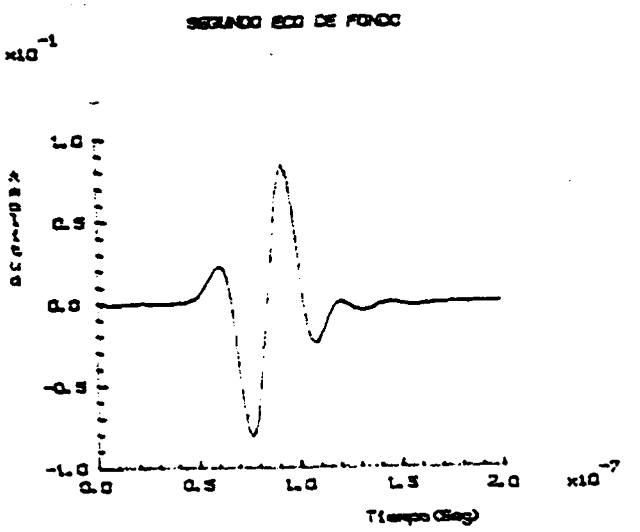

Fig. 9
Steel sample. 2nd backwall echo

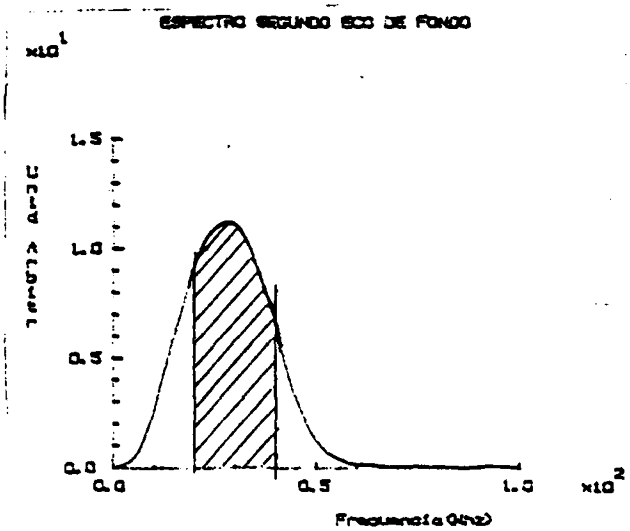

Fig. 10
Spectrum of signal of fig. 9

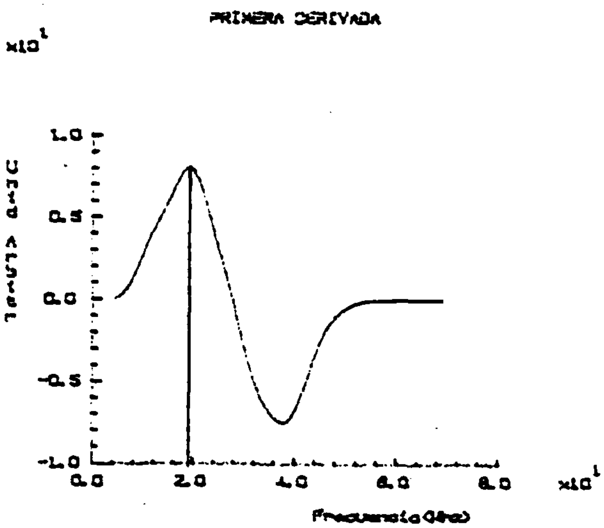

Fig. 11
First derivative

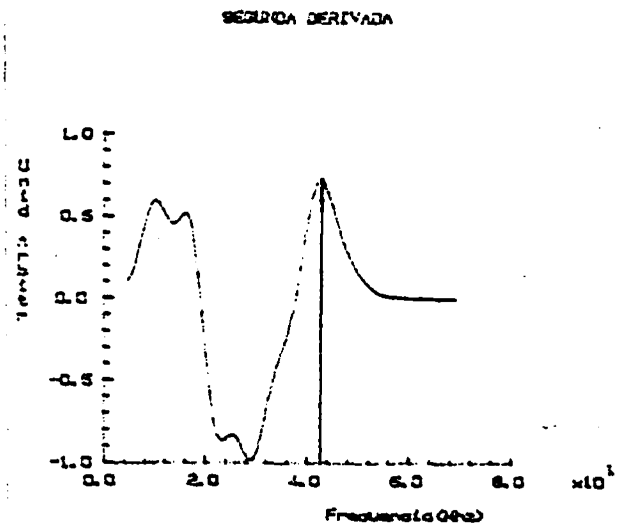

Fig. 12
Second derivative

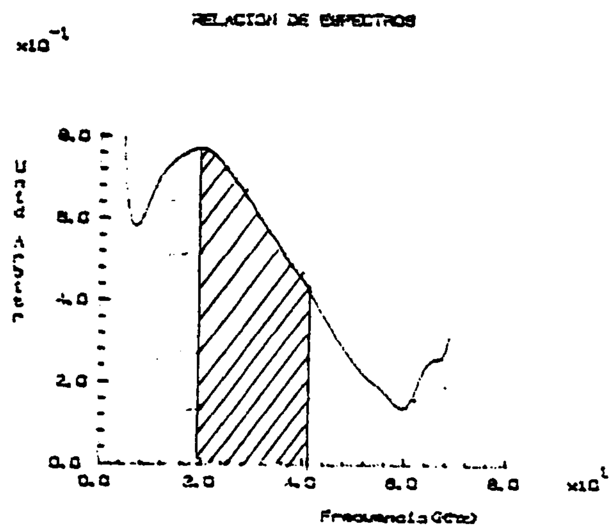

Fig. 13
Ratio of spectra of fig. 8 and 10

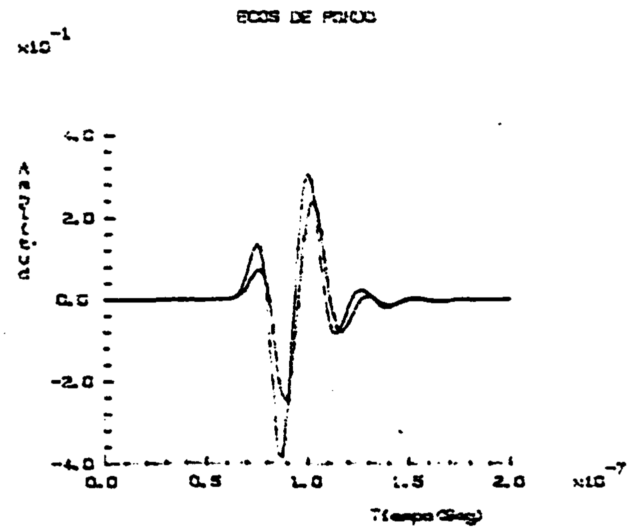

Fig. 14
Quenched steel

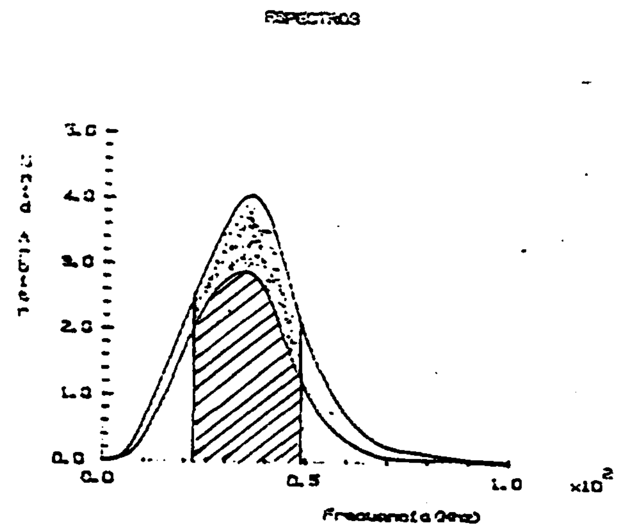

Fig. 15
Spectra of signals of fig. 14

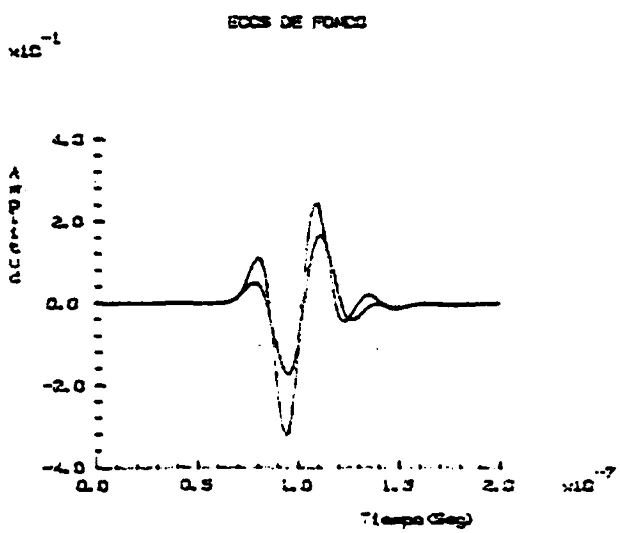

Fig. 16
Annealed steel

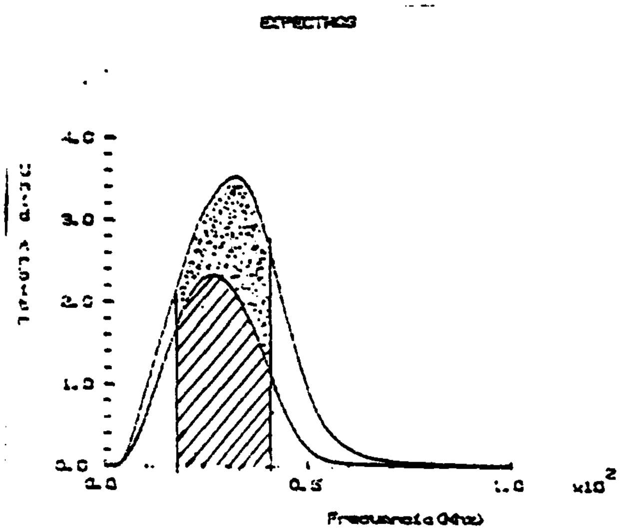

Fig. 17
Spectra of signals of fig. 16

A-4/002.3 Imprenta del INTA

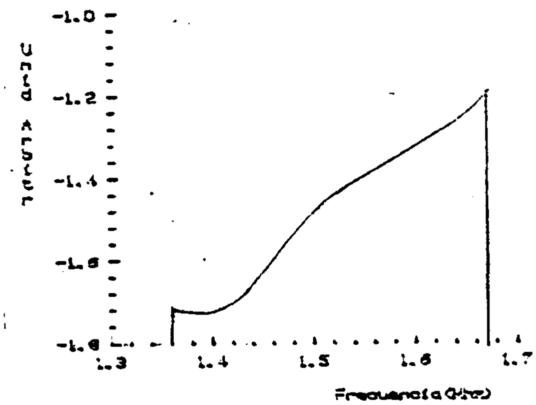

Fig. 18
Quenched sample

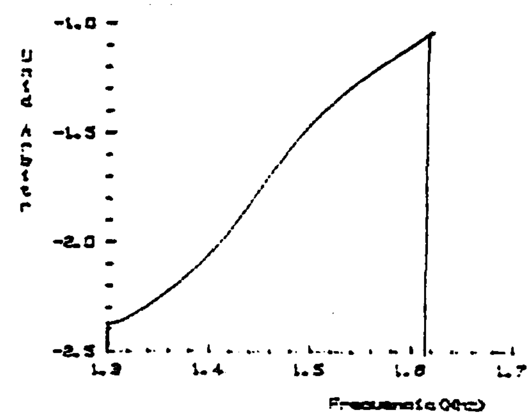

Fig. 19
Annealed sample

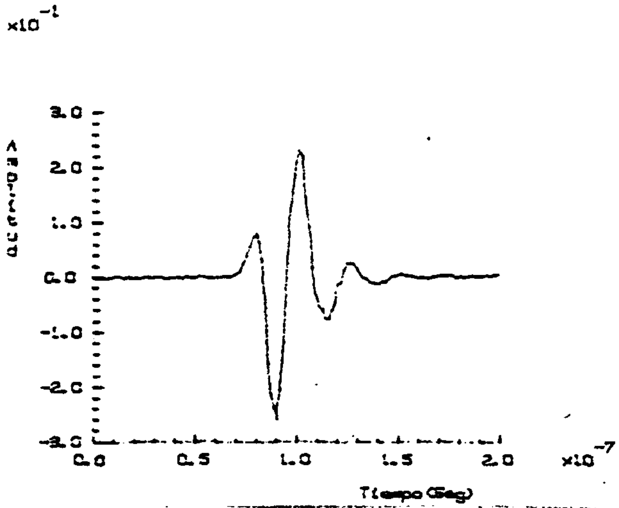

Fig. 20
10 samples averaged

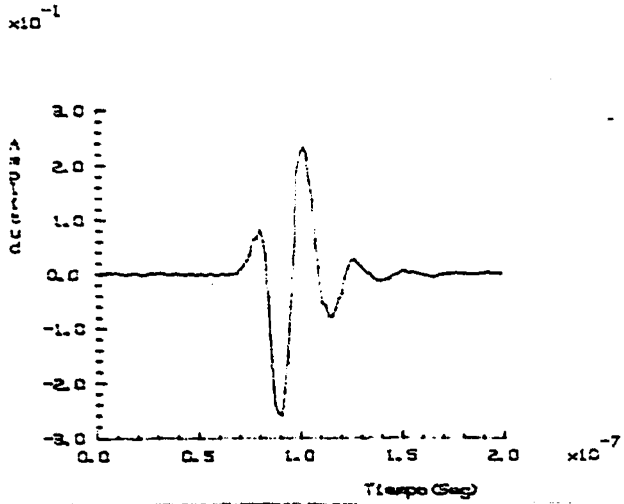

Fig. 21
Same as Fig. 20, other test

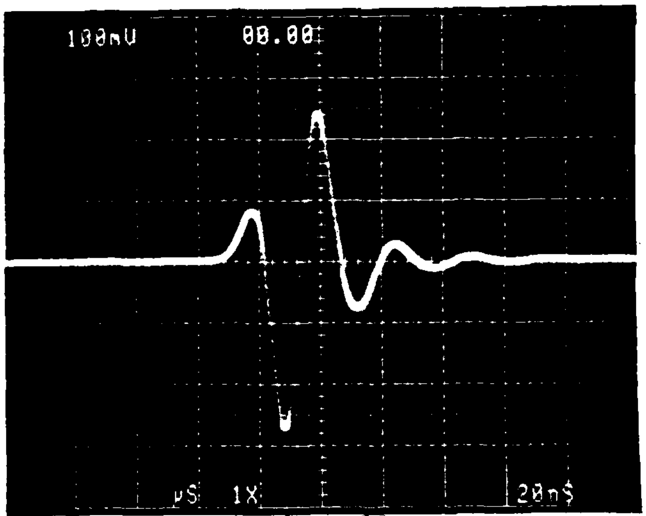

Fig. 21 a
Analog signal

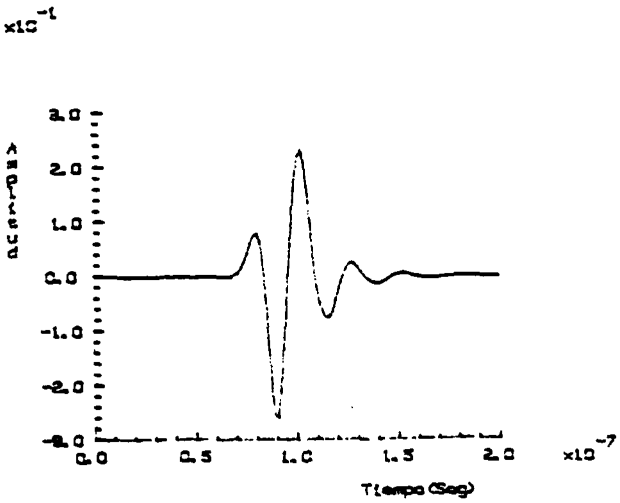

Fig. 22
Some signals as fig. 22, but 150 averaged samples

A-6/002.3 Imprenta del INTA

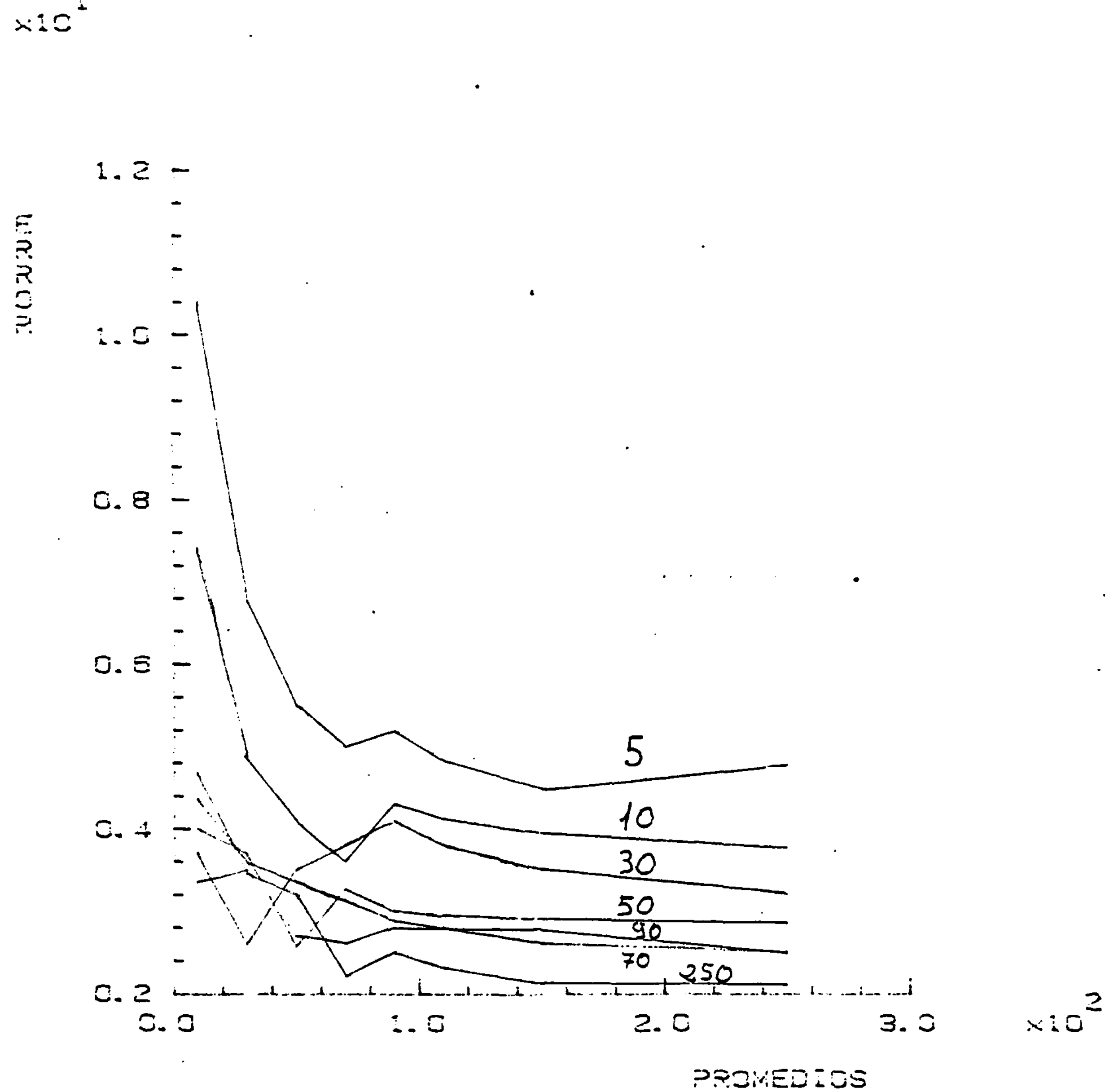

Fig. 23
Effect of number of averaged samples on error magnitude.

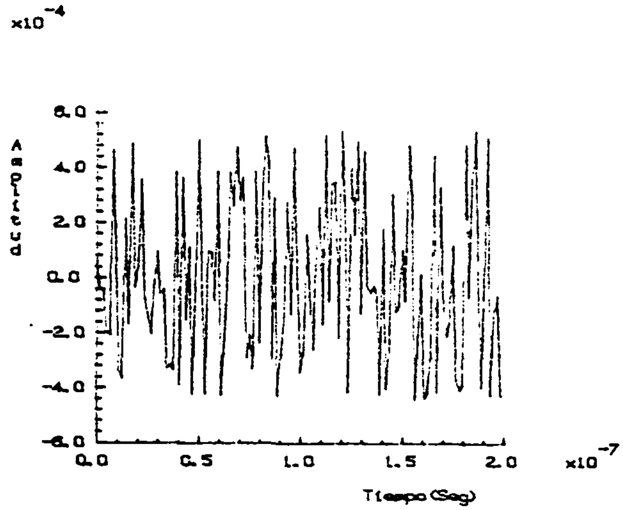

Fig. 24
Computer generated random noise

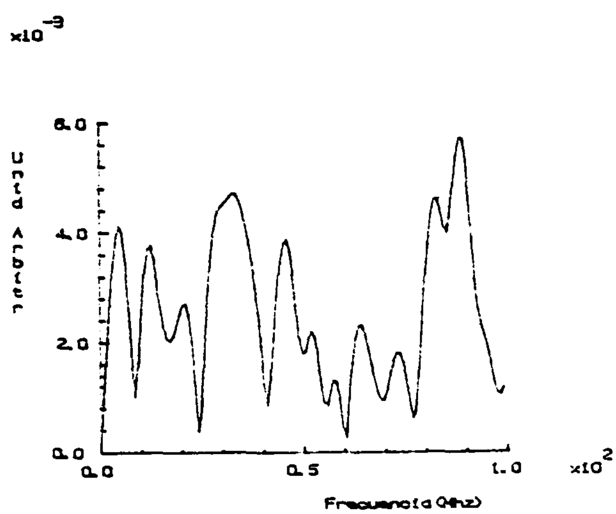

Fig. 25
Spectrum of noise of fig. 24

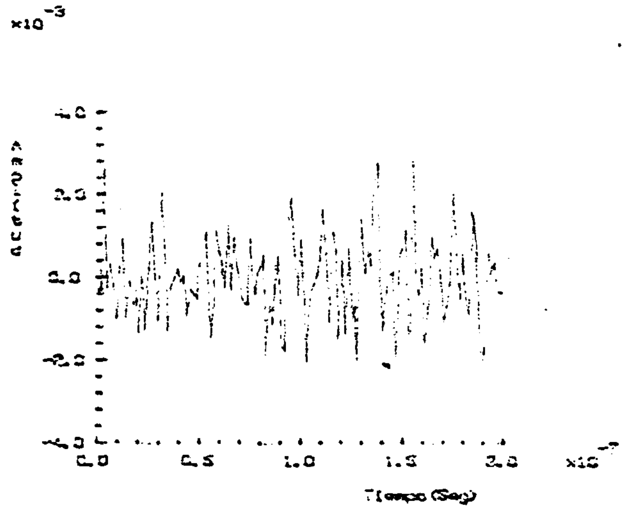

Fig. 26
Time base digitization, 10 averaged samples.

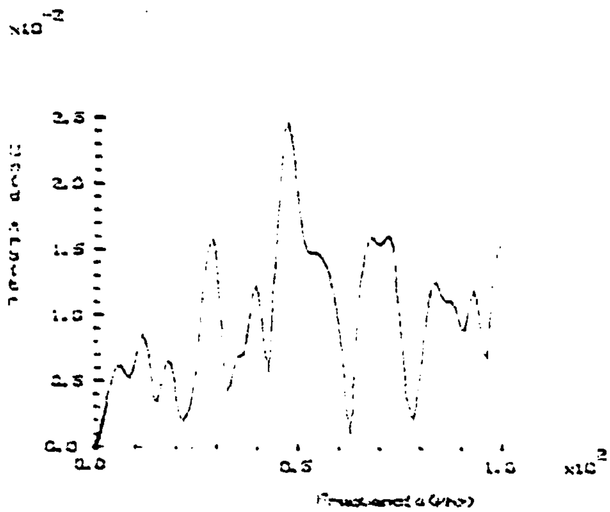

Fig. 27
Spectrum of signal of fig. 26

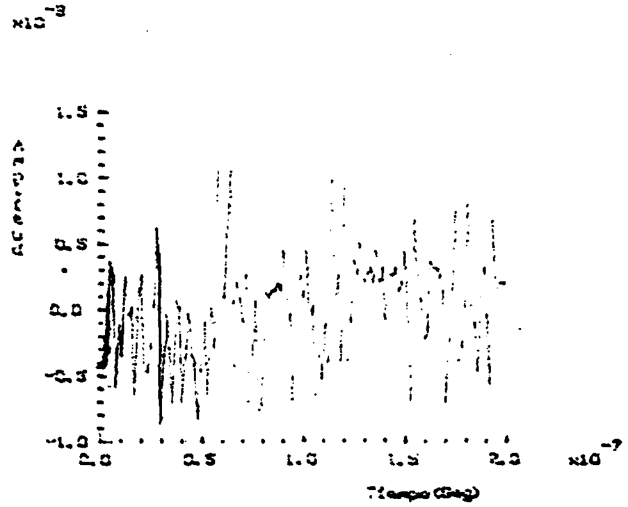

Fig. 28
Time base digitization. 50 averaged samples.

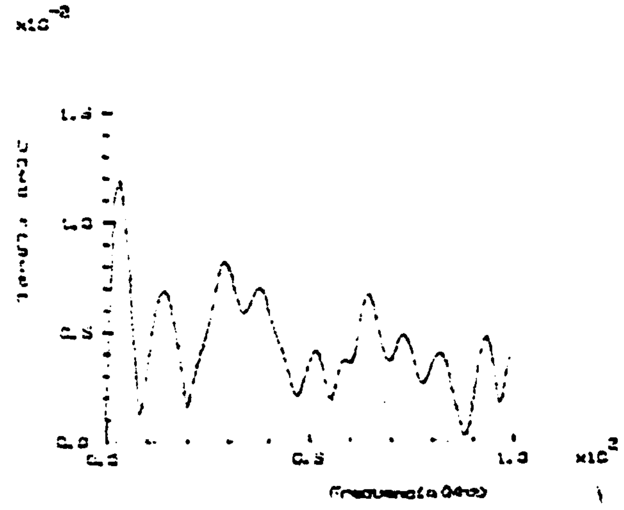

Fig. 29
Spectrum of signal of fig. 28

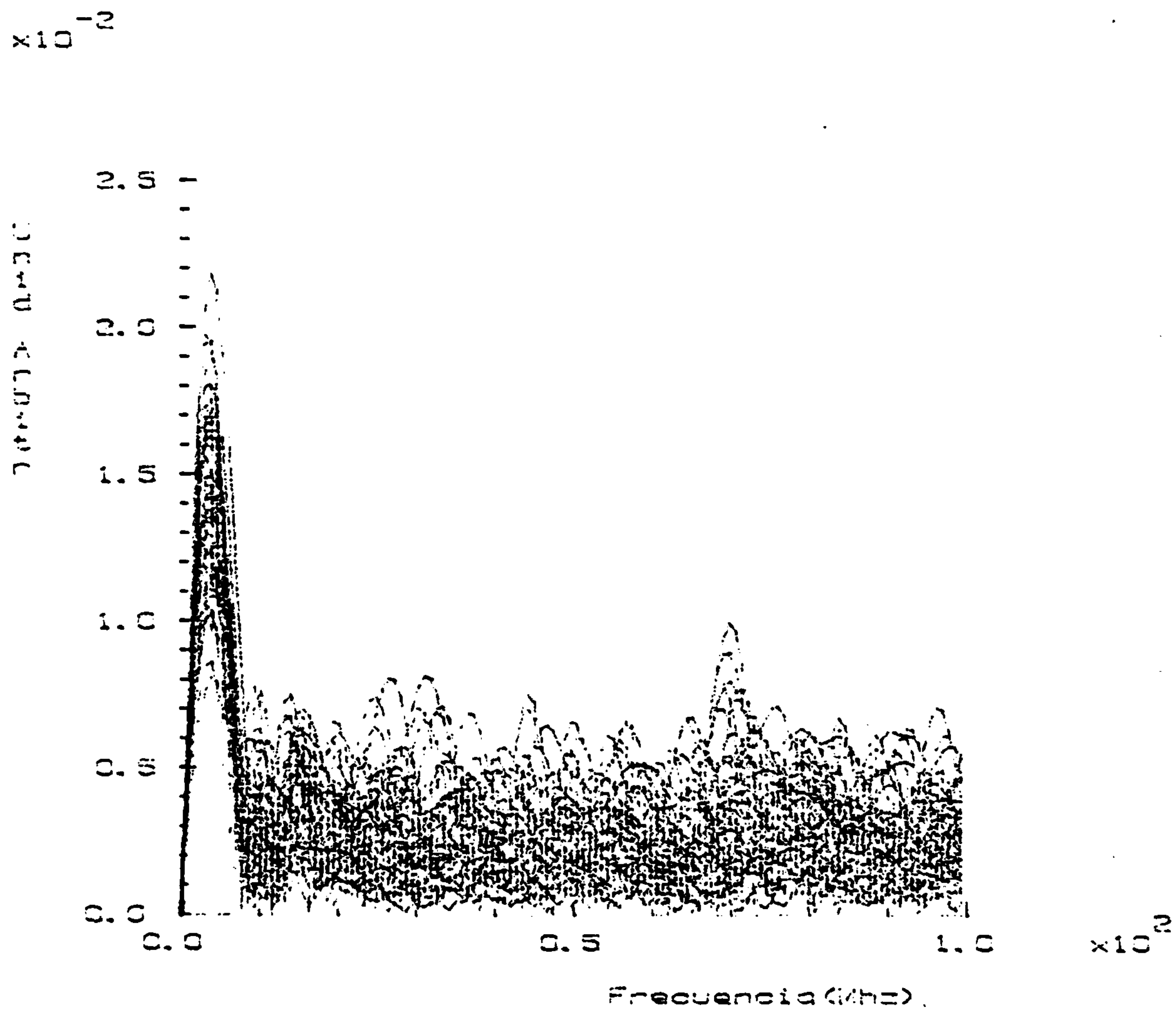

Fig. 30
50 overlapped of spectra of signals like that of fig. 28.

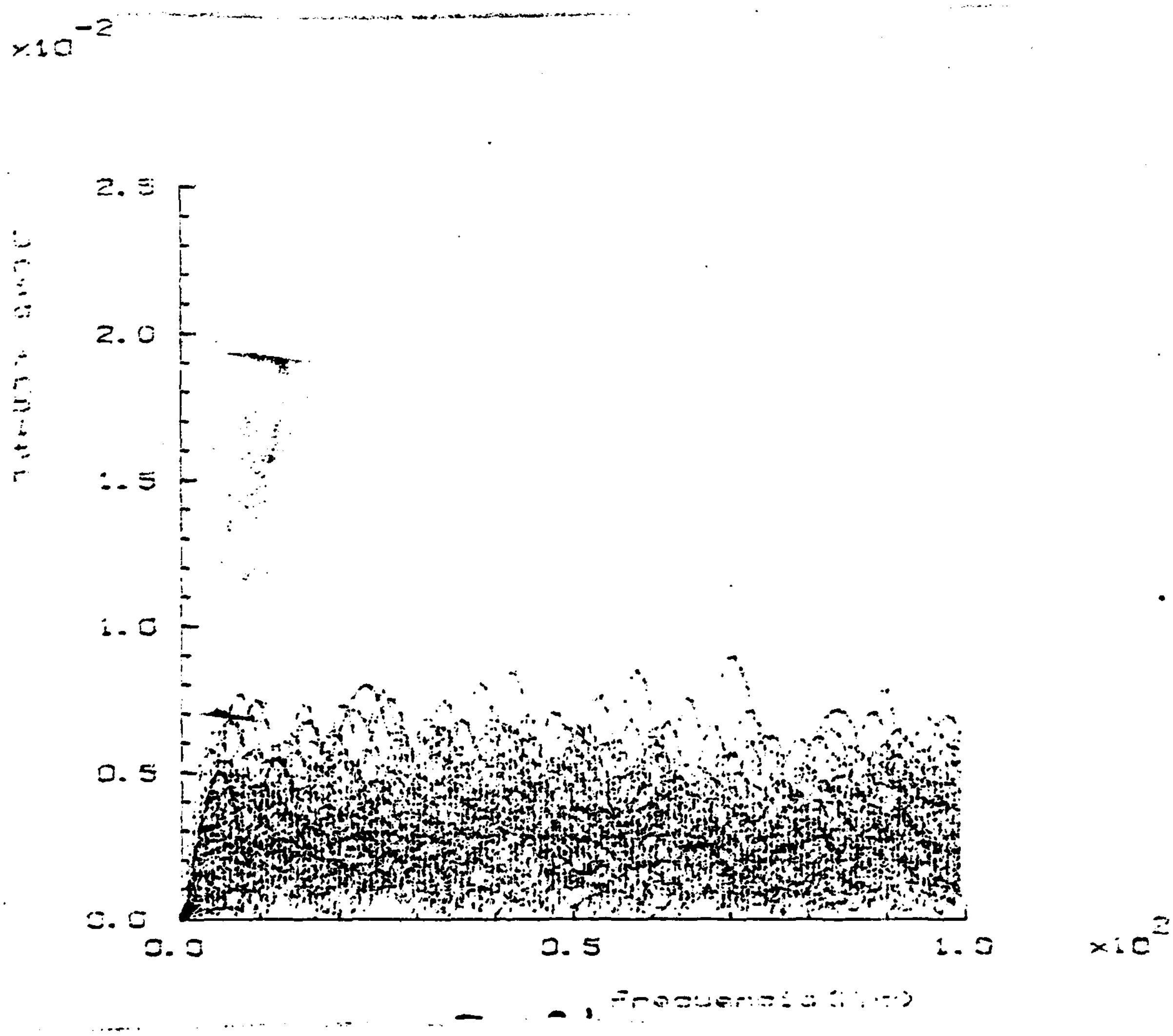

Fig. 31
50 overlapped spectra of random noise (fig. 24).

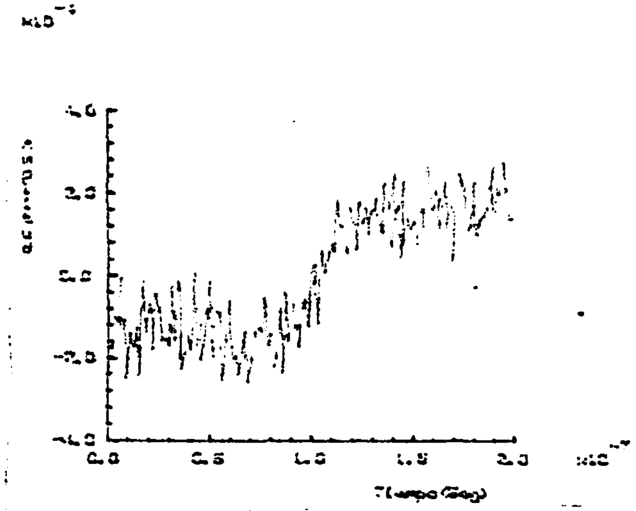

Fig. 32
Time base digitization. 50 x 50
averaged samples.

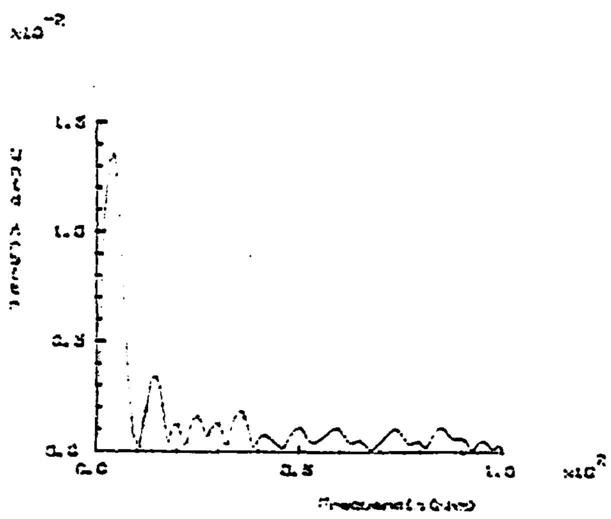

Fig. 33
Spectrum of signal of fig. 32.

A-4/002.3 Imprenta del INTA

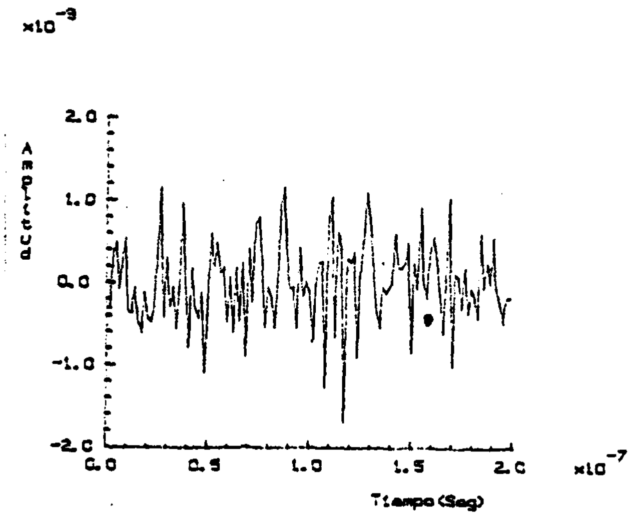

Fig. 34
Time base digitization. 10 averaged samples.

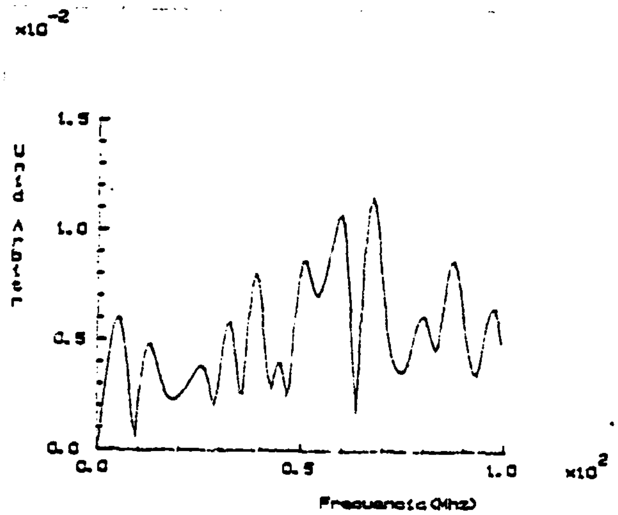

Fig. 35
Spectrum of signal of fig. 34

A-4/002.3 Imprenta del INTA

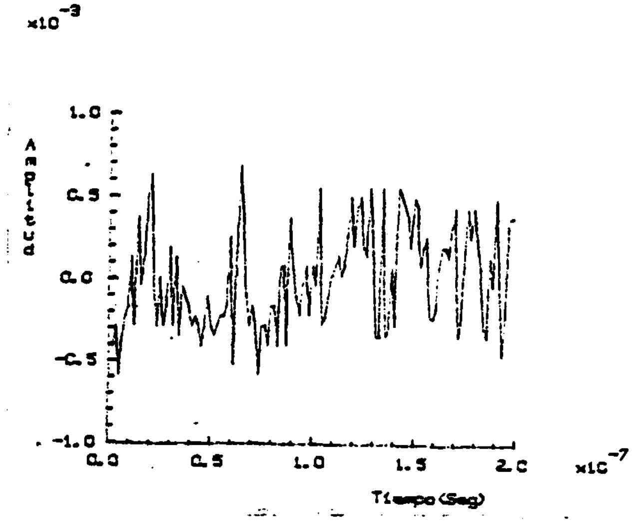

Fig. 36
Time base digitization. 50 averaged samples.

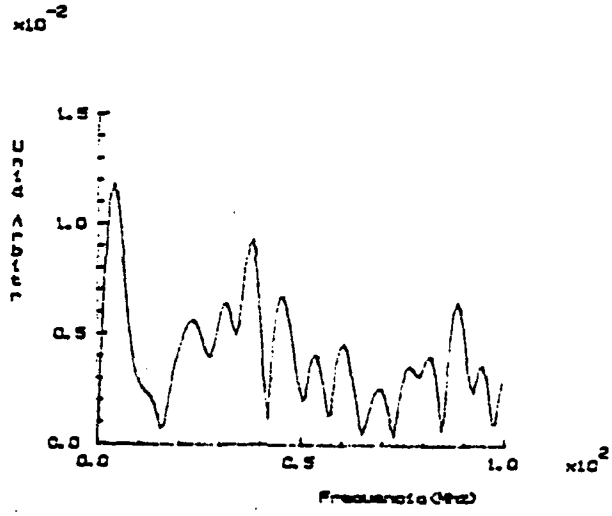

Fig. 37
Spectrum of signal of fig. 36

A-1/062.3 Imprenta del INTA

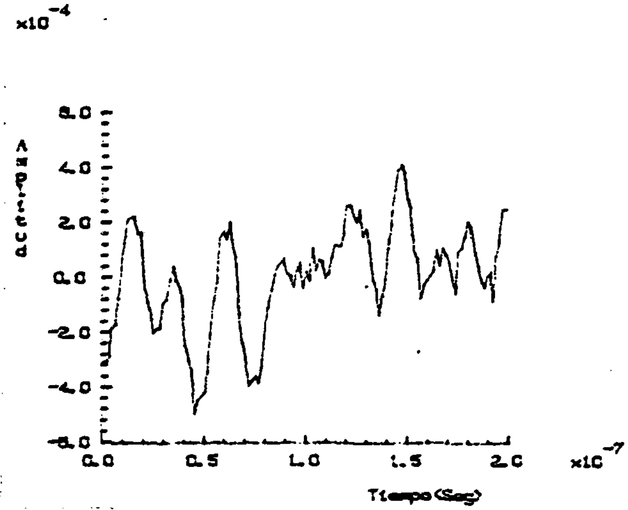

Fig. 38
Time base digitization. 50 x 50 averaged samples.

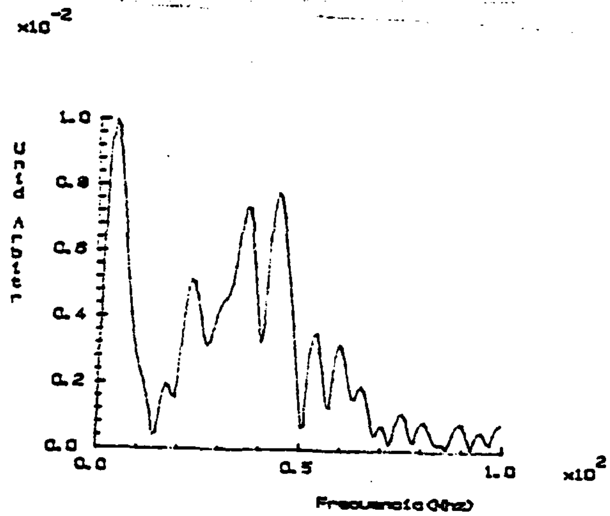

Fig. 39
Spectrum of the signal of fig. 38

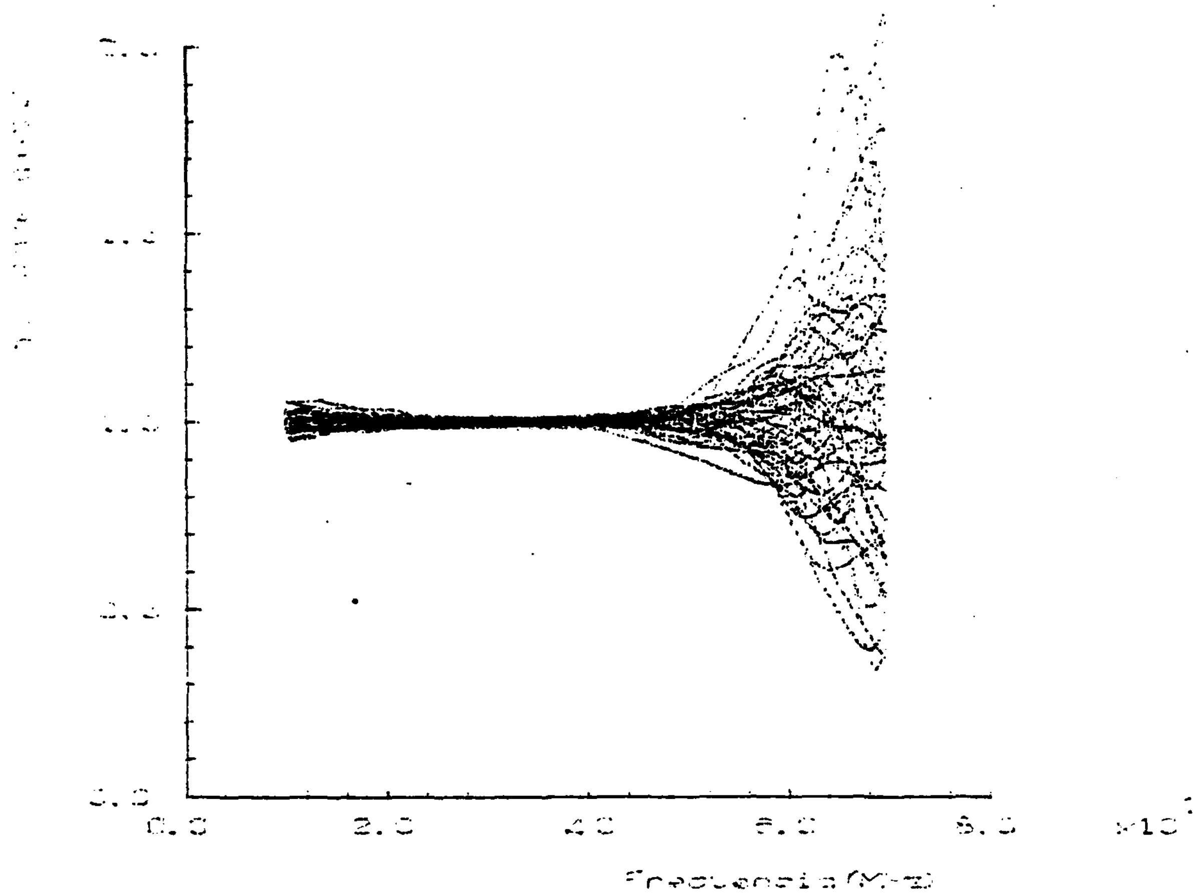

Fig. 40
Ratio of spectra of the same analog signal. Each curve is the ratio of two succesive spectra. Experiment repeated 50 times.

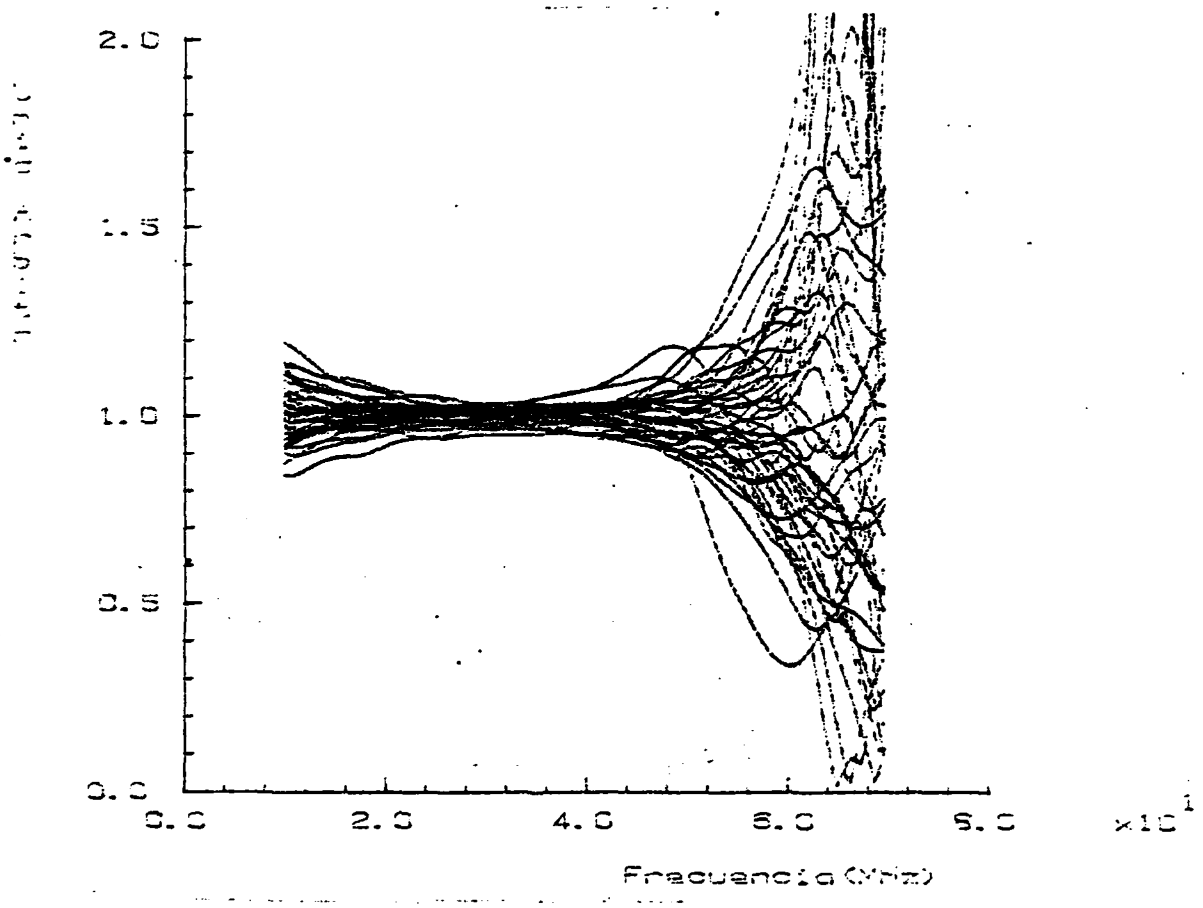

Fig. 41
Ratio of spectra of signal with jitter.
Spreading is higher than in fig. 40.

A-1/002.3 Imprenta del INTA

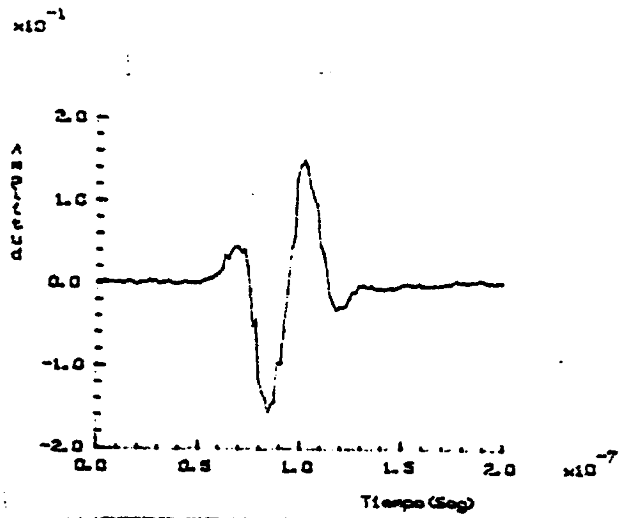

Fig. 42
Signal with jitter digitization 10 averaged samples.

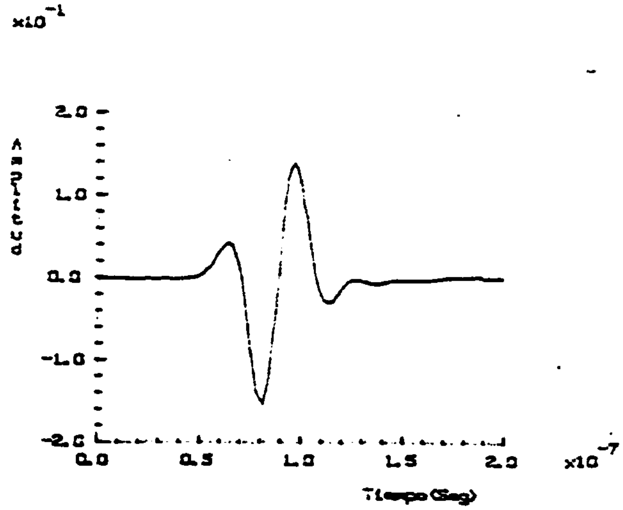

Fig. 43
Same of fig. 42. 100 averaged samples.

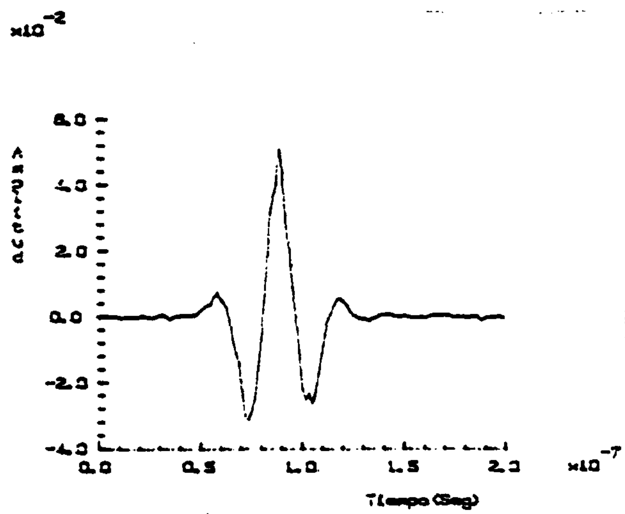

Fig. 44
Derivative of signal of fig. 43.

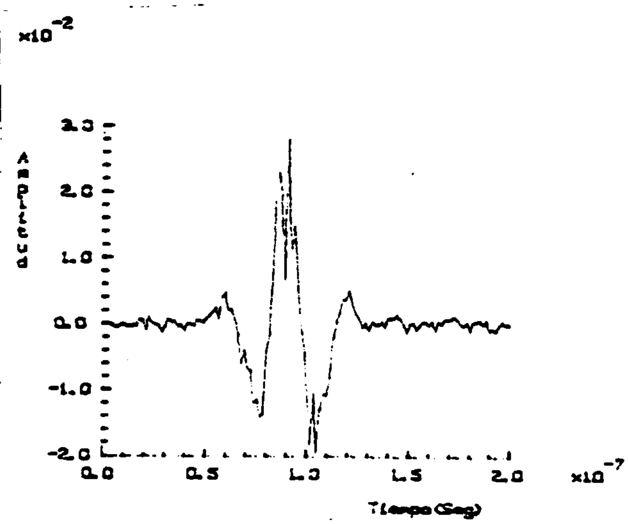

Fig. 45
Difference between two successive digitization of the same signal.

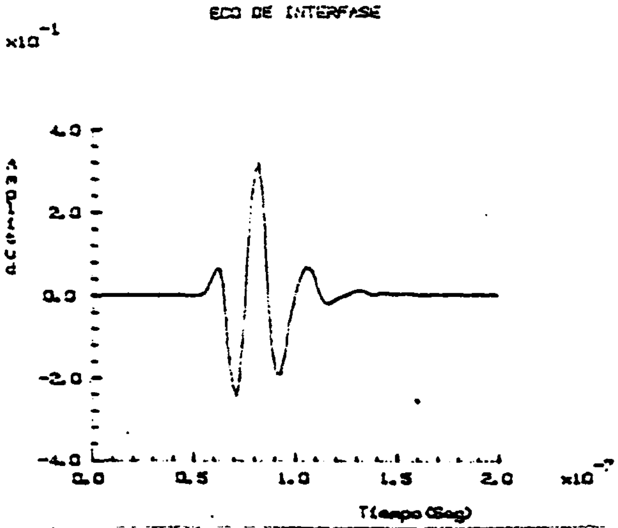

Fig. 46

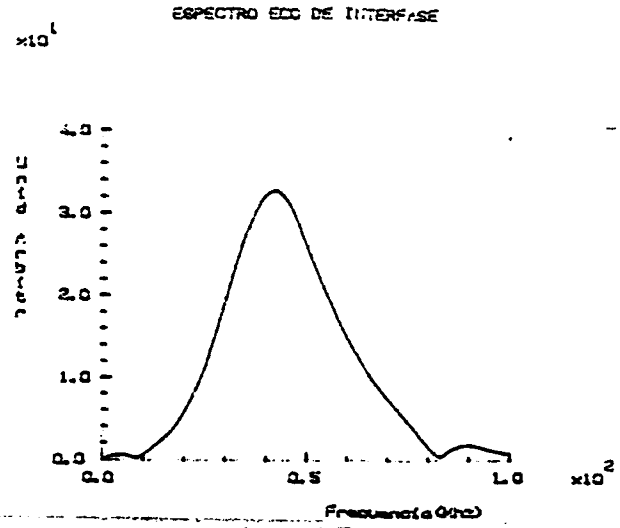

Fig. 47

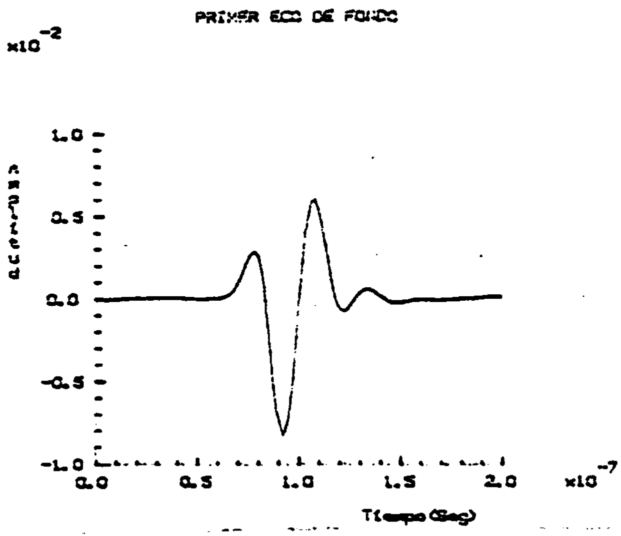

Fig. 48

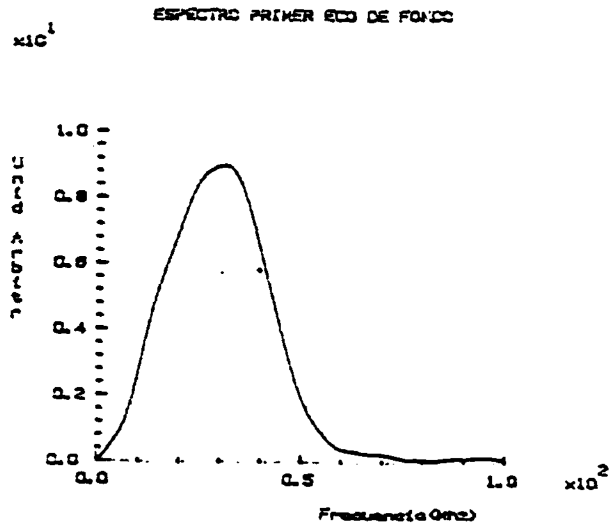

Fig. 49

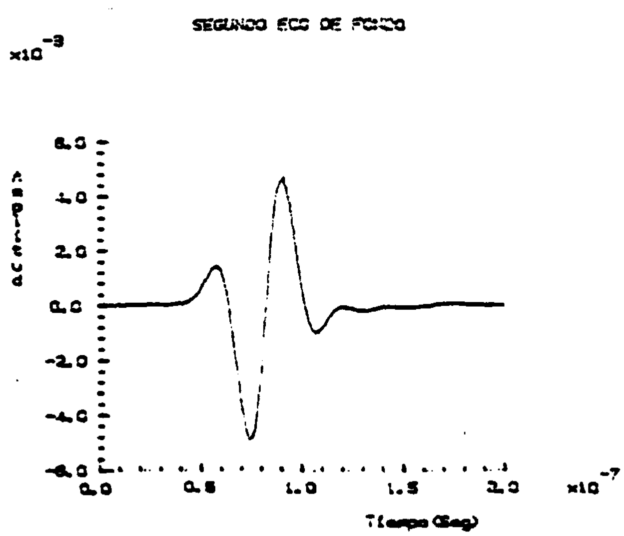

Fig. 50

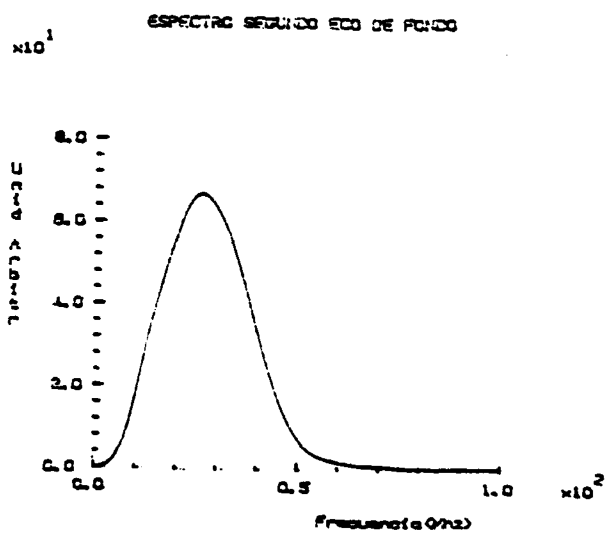

Fig. 51

Three echoes method

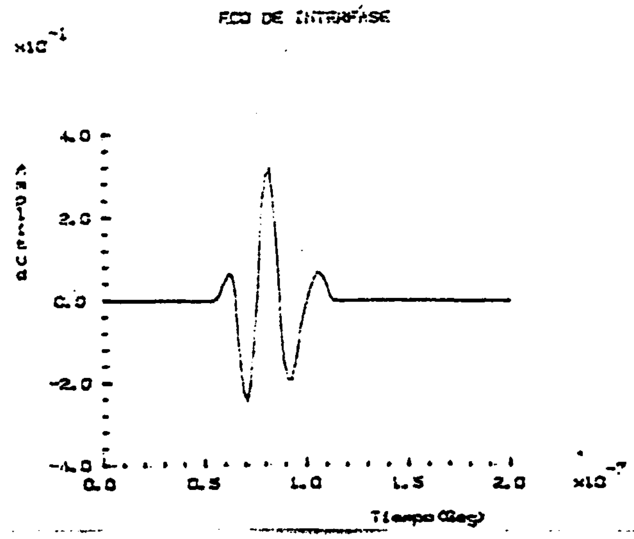

Fig. 52

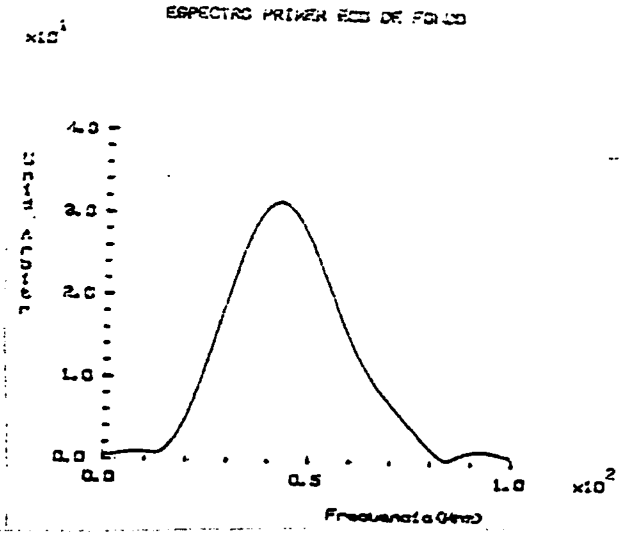

Fig. 53

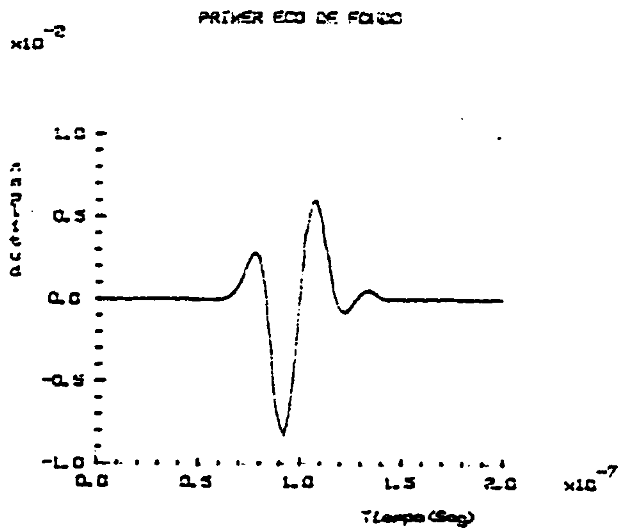

Fig. 54

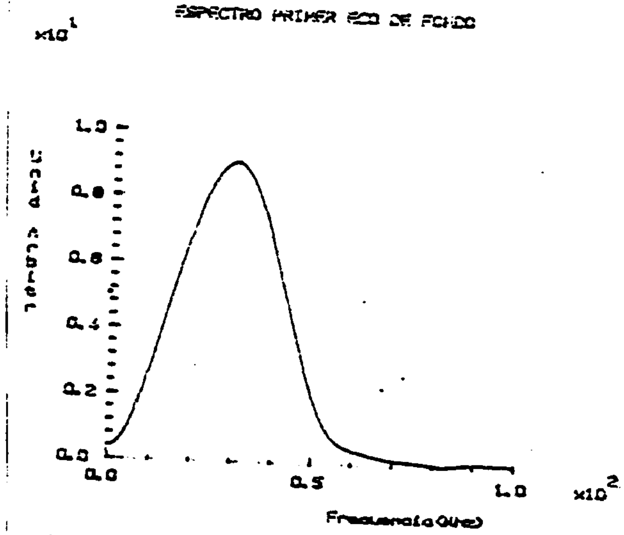

Fig. 55

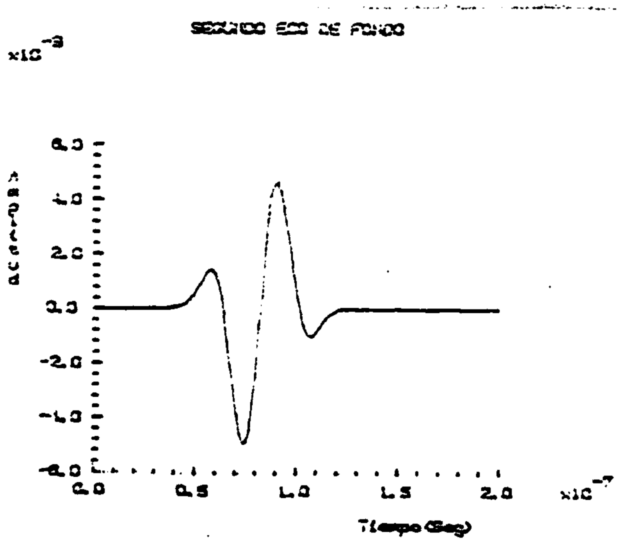

Fig. 56

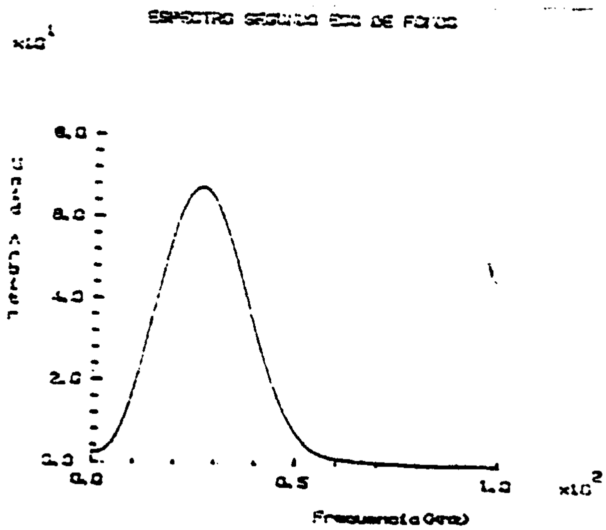

Fig. 57

Three echoes method. Truncated signals (compare with preceding figure).

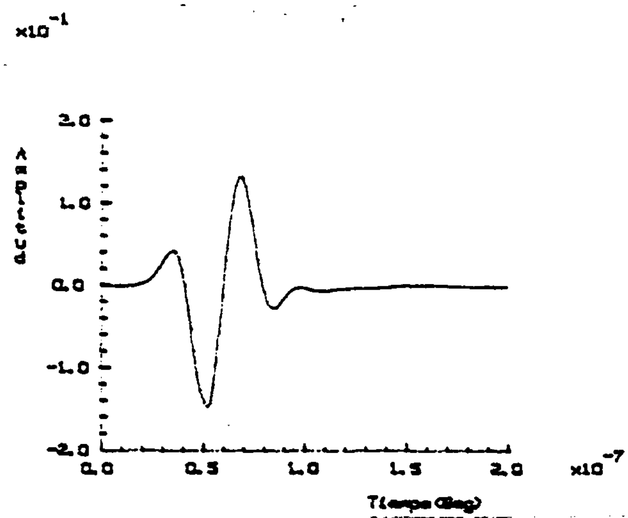

Fig. 58
Original signal

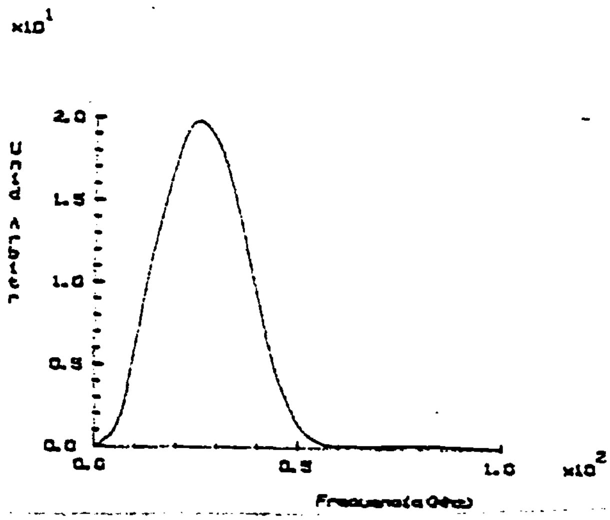

Fig. 59
Spectrum of signal of fig.58

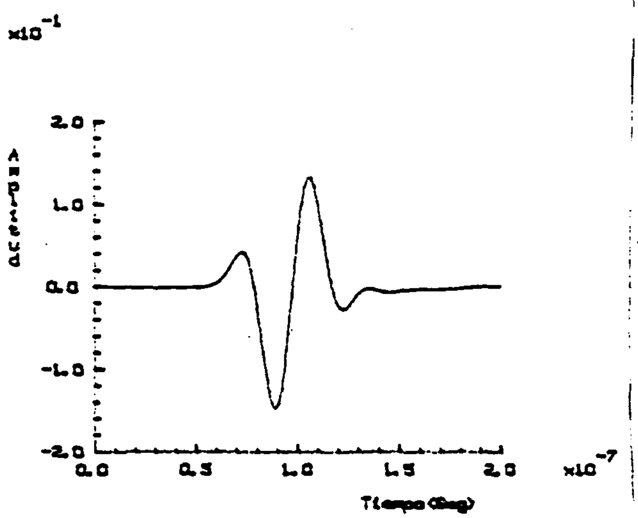

Fig. 60
Displaced original signal

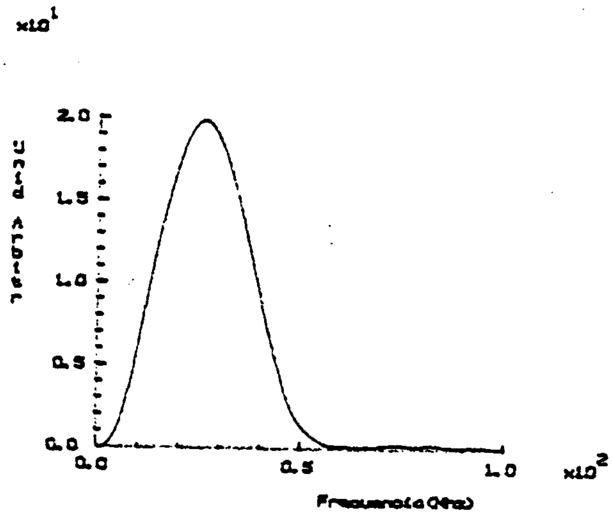

Fig. 61
Spectrum of signal of fig.60

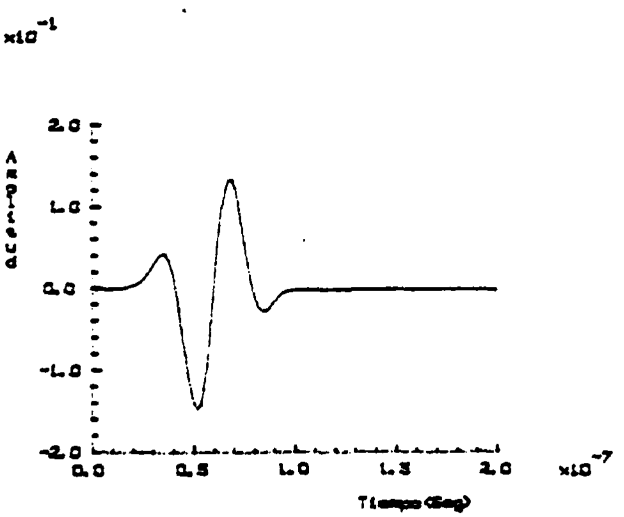

Fig. 62
Truncated original signal

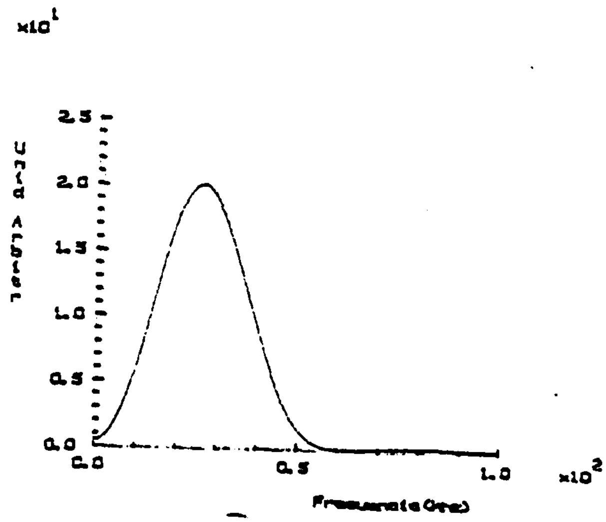

Fig. 63
Spectrum of signal of fig.62